Journal of Engineering Mathematics **41:** 117–144, 2001.

Operating charts for continuous sedimentation I: Control of steady states

STEFAN DIEHL
School of Technology and Society, Malmö University, S-205 06 Malmö, Sweden (e-mail: Stefan.Diehl@ts.mah.se)

Received 11 April 2000; accepted in revised form 8 January 2001

Abstract. The industrial process of continuous sedimentation of solid particles in a liquid takes place in a clarifier-thickener unit, which is a large tank with a feed inlet somewhere in the middle and outlets at the top and bottom. For half a century the constitutive assumption by Kynch has provided a platform from which steady-state mass-balance considerations have been used to obtain rules and graphical tools for prediction of steady-state situations, design and control. This is often referred to as the 'solids-flux theory' containing such key words as the 'operating line', 'state point' and 'limiting flux'. The basic assumptions of the solids-flux theory yield a nonlinear partial differential equation that models the entire process. Since unique physically relevant solutions can now be obtained, the knowledge of these is used to establish and extend the solids-flux theory. Detailed information on all steady-state solutions and the control of these by adjusting a volume flow is presented by means of operating charts. Most of these are concentration-flux diagrams with information on, for example, how to perform a control action to fulfil a certain control objective formulated in terms of the output variables in steady state.

Key words: operating charts, continuous sedimentation, settling, thickener, solids-flux theory

1. Introduction

The industrial process of continuous sedimentation of solid particles in a liquid takes place in a clarifier-thickener unit, which is a large tank having one feed inlet somewhere in the middle and outlets at the top and bottom. It is used, for example, in the mineral industry and waste-water treatment plants. Gravity sedimentation alone is a nonlinear process with discontinuities in the concentration profile. The volume flows of the inlet and outlets in continuous sedimentation entail that there is an additional nonlinear phenomenon that makes the behaviour even more complicated to predict and control. These facts imply that the mathematical modelling is difficult and substantial simplifications still have to be made. However, the need for information to the operators of the plants has led to the development of rules, operating charts and graphical tools based on experiments and physical considerations in parallel to the development of mathematically rigorous descriptions of the process by partial differential equations.

1.1. Previous works within the solids-flux theory

As early as 1916 the influence of the concentration on the settling velocity was noticed by Coe and Clevenger [1], who gave a formula for the minimum cross-sectional area required for the thickener to work properly. The formula is a mass balance for the thickener in steady-state operation involving the underflow discharge concentration, and the concentration and its corresponding settling velocity in the lower part of the vessel. Different procedures for the

design of thickeners presented later contain essentially the same information, see Vesilind [2], Concha and Barrientos [3] and references therein.

In the pioneering work by Kynch [4] the method of characteristics was used to produce solutions of the continuity equation, or conservation law, where the constitutive assumption is that the settling velocity is a function of the concentration only. This assumption is valid for ideal mono-sized particles that do not show any compressible behaviour and for which diffusion phenomena are neglected; *cf.* experiments reported in [5–7]. Kynch's assumption, together with the conservation of mass in one dimension, has provided a platform called the *solids-flux theory* from which many conclusions have been drawn. Graphical constructions by using the batch-flux curve for obtaining concentrations in steady-state operation were initiated by Yoshioka *et al.* [8] and developed by Jernqvist [9–11]. Unfortunately, Jernqvist's results do not seem to have reached other researchers. Similar developments, but not as extensive, were made in the '60s and '70s by, for example, Hasset [12], Dick [13] and McHarg [14]. Concepts such as the operating line, the limiting flux and the state point (pivot point, feed point) were used in the flux theory to describe steady-state situations; see also [15, 16], [17, Chapter 5], [18, 19]. Further interpretations concerning clarification failure and control were made in the '70s and '80s by Keinath, Laquidara *et al.* [20–22] and a chart describing steady states was presented by Lev *et al.* [23]. Up to now the need for the flux theory and graphical constructions for describing the process has been apparent; see *e.g.* [24–31]. The results presented in this context have been obtained by direct physical considerations, mainly mass balances, and the fundamental results were presented in 1965 by Jernqvist [10, 11].

1.2. Related works

The advantage of the Kynch assumption is the possibility of constructing analytical solutions of the conservation law, or continuity equation. The concentration is constant along the characteristics, which are straight lines. As they intersect, a discontinuity, or shock wave, is formed. Its speed is governed by the jump condition (conservation of mass), see Lax [32]. The entropy condition by Oleinik [33] ensures a unique and physically relevant solution for given initial data. The construction of solutions by the method of characteristics describing sedimentation in the thickening zone (below the feed level) or in batch mode can be found in [34], [35, Chapter 6.7], [36–39].

Analyses of the entire clarifier-thickener unit having a varying cross-sectional area by a nonlinear partial differential equation with point source and discontinuous flux function were made independently and with different approaches by Chancelier *et al.* [40] and the author in [41, 42]. To put it in a nutshell, Chancelier *et al.* smooth the discontinuities in the flux function (and the point source) so that Oleinik's entropy condition can be used. In [43] Chancelier *et al.* relate their previously obtained results to the solids-flux theory and present, among other things, a chart describing steady-state solutions.

In [41] the author presented a generalized entropy condition, which, for given initial data, enables construction of the unique physically relevant solution of the entire process by the method of characteristics, see [42, 44]. The solution is physically relevant in the sense of viscosity solutions of a parabolic equation obtained when a small diffusion term is added to the original hyperbolic equation in addition to the smoothing of the flux function, see [45, 46]. This entropy condition and the unique solutions enable a rigorous description of the solids-flux theory and are crucial for the results of the present paper. The steady-state solutions have been presented in [42, 47] and are classified in Section 3.2 in terms of a steady-state chart in

the case of a constant cross-sectional area. If the cross-sectional area is varying, a more refined chart can be obtained. The analysis then contains more technical details. The difference in the behaviour of the process, however, is only substantial if the cross-sectional area decreases rapidly with depth, see [44]. In this paper we confine ourselves to a constant cross-sectional area.

The analysis of steady-state solutions by Lev *et al.* [23] is based on physical considerations on mass balances, discussions on the continuity equation with and without a small diffusion term and on some assumptions on the solution of these equations, *e.g.* on monotonicity, stability and that the concentration is constant within the clarification and thickening zone (for the hyperbolic equation), respectively. They present a steady-state chart with the same five regions as in the present paper. The reason for this agreement is that their assumptions were correct for the solutions corresponding to the interior of the five regions. As is shown in the present paper, the solutions corresponding to the boundaries of these five regions may have discontinuities within the clarification and thickening zone, which is important for the operation and control of the clarifier-thickener unit.

It should be emphasized that many real flocculated suspensions show a compressible behaviour at high concentrations. Under normal operating conditions there is a compression zone at the bottom of the thickener within which the process can be modelled by a parabolic equation. The sedimentation process can then be modelled by a degenerate parabolic conservation law. This has been studied extensively lately by, among others, Bürger and co-workers, see [48, 49], [50, Chapters 9 and 10] and the references therein. Numerical calculations are needed to obtain quantitative information already in the batch-sedimentation case for any initial data. This is one reason why the present paper only deals with the hyperbolic model, for which exact solutions can be constructed. Another one is the fact that the behaviour of the degenerate parabolic model for arbitrary loading conditions in continuous sedimentation is not yet analysed mathematically. A third reason – and the most important one – is to establish the solids-flux theory and extend this in the direction of the control of the steady states.

1.3. The aims of the paper

Given the ideal assumptions of the solids flux theory:

- the conservation of mass in one dimension,
- the Kynch constitutive assumption,

the theory of nonlinear conservation laws (with boundary relations satisfying the conservation of mass) yields all possible steady-state solutions for the entire clarification-thickening process. These are obtained in previous papers by the author and constitute the theoretical starting-point of the present paper. The focus is thus on the influence the volume flows of the inlet and outlets have on the process of *continuous* sedimentation rather than on the modelling of the batch sedimentation-consolidation process. The aims are the following:

1. Establish unique answers to the issues raised in the literature concerning the description of the steady-state solutions. Extend the solids-flux theory to cover all theoretically possible loading conditions. This comprises explicit formulae, a steady-state chart and graphical constructions.
2. Introduce concepts and establish results on the dependence of the steady-state solutions on the commonly used control variable: the volume flow of the underflow.

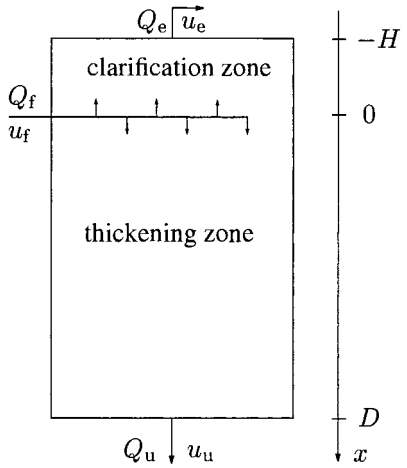

Figure 1. Schematic picture of an ideal one-dimensional clarifier-thickener unit.

3. Discuss system purposes and suggest control criteria and objectives with respect to the steady-state solutions. Present results on how to obtain the control objectives and what the limitations are.
4. Obtain a better understanding and feeling of the nonlinear process by presenting the results in terms of operating charts.

The rest of the paper is organized as follows: Section 2 reviews the mathematical model of an ideal one-dimensional clarifier-thickener unit, the Kynch assumption and the notation necessary for describing the steady-state solutions. Section 3 deals with the first aim above. The second and the third aims are considered in Section 4 and the proofs are presented in the Appendix. An example is provided in Section 5, and discussion and conclusions can be found in Section 6.

2. A model of continuous sedimentation

2.1. THE CLARIFIER-THICKENER UNIT

Continuous sedimentation of solid particles in a liquid takes place in a clarifier-thickener unit or settler, see Figure 1. Let $u(x,t)$ denote the concentration (mass per unit volume) at depth x and time t. The height of the clarification zone is denoted by H and the depth of the thickening zone by D. At $x = 0$ the settler is fed with suspended solids at a known concentration $u_f(t)$ and at a known constant flow rate $Q_f > 0$ (volume per unit time). When considering steady-state solutions, we assume that $u_f > 0$. Otherwise, only the trivial zero solution applies. A high concentration of solids is taken out at the underflow, at $x = D$, at a flow rate Q_u. It is assumed that $0 < Q_u \leq Q_f$. The effluent flow Q_e, at $x = -H$, is consequently defined by $Q_e = Q_f - Q_u \geq 0$. The cross-sectional area A of the settler is assumed to be constant and the concentration u is assumed to be constant on each cross-section. The effluent and underflow concentrations, $u_e(t)$ and $u_u(t)$, are unknown. We define the bulk velocities in the thickening and clarification zone as

$$q_u = \frac{Q_u}{A}\,, \qquad q_e = \frac{Q_e}{A}\,,$$

respectively, hence q_e is positive upwards. Of course, the volume flows may depend on time, but this is not written out explicitly. The volume flow of the underflow Q_u is the control variable of the process, and we assume that this flow can be adjusted by a pump. In Sections 2 and 3 Q_u is considered to have a fixed, but arbitrary, value. In Section 4, which deals with the control of steady states, the dependence on the control variable of all quantities is written out explicitly.

2.2. KYNCH'S ASSUMPTION AND CHARACTERISTIC CONCENTRATIONS

According to the constitutive assumption by Kynch [4] the settling velocity of the solids due to gravity in a batch settling column is a function of the local concentration only, $v_{settl}(u)$. The maximum packing concentration is denoted by u_{max}. The batch-settling flux (mass per unit time and unit area) is denoted by $f_b(u) = v_{settl}(u)u$ and is assumed to satisfy

$$\begin{aligned} &f_b \in C^2[0, u_{max}] , && f_b(u) > 0 , \quad 0 < u < u_{max} , \\ &f_b(0) = f_b(u_{max}) = 0 , && f_b \text{ has an inflection point } u_{infl} \in (0, u_{max}) , \\ &f_b''(u) < 0, \quad u \in (0, u_{infl}) , && f_b''(u) > 0 , \quad u \in (u_{infl}, u_{max}) , \end{aligned} \tag{1}$$

see Figure 2. In continuous sedimentation the volume flows Q_u and Q_e give rise to the flux terms $q_u u$ and $-q_e u$, respectively, which are superimposed on the batch-settling flux to yield

$$\begin{aligned} g(u) &= f_b(u) - q_e u , \qquad -H < x < 0 , \\ f(u) &= f_b(u) + q_u u , \qquad 0 < x < D . \end{aligned}$$

see Figure 2. The form of the batch-settling flux function f_b and the two volume flows Q_u and Q_e imply that there are certain characteristic concentrations that appear in the solutions. Because of Lemma 1 (in the Appendix) we can define $u_z > 0$ as the unique positive zero of g, *i.e.*, $g(u_z) = 0$; *cf.* Figure 2. (If Q_e is so large that $g(u) < 0$ for all $u > 0$, we define $u_z = 0$, which implies simplifications in the analysis. This corresponds to an extreme case, which is probably not of interest in the application.) The concentration u_z is such that the gravity settling downwards is balanced by the bulk flow upwards. Hence, a layer of solids in the clarification zone with this concentration will be at rest. Define

$$\bar{q}_u = -f_b'(u_{max}) \quad \text{and} \quad \bar{\bar{q}}_u = -f_b'(u_{infl}) ,$$

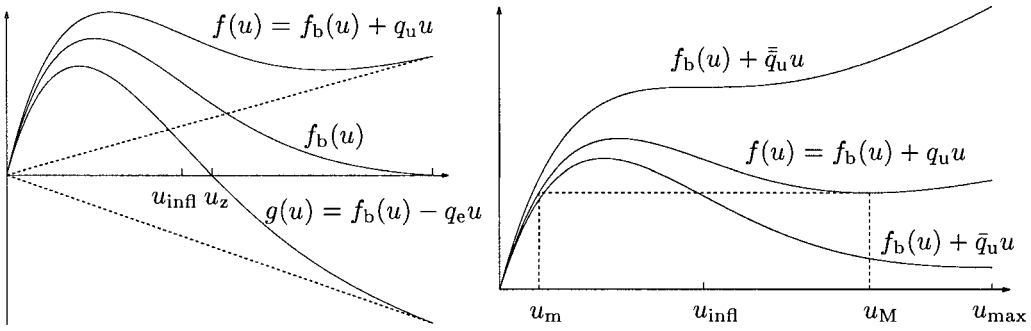

Figure 2. Flux curves and characteristic concentrations. Note that $f_b(u)$, $f(u)$ and $g(u)$ have the same inflection point u_{infl}.

which are the bulk velocities such that the slope of f is zero at $u_{\max}$ and u_{infl}, respectively, see Figure 2. The local minimizer, denoted u_{M}, on the right of u_{infl} plays an important role in the behaviour of the process. For intermediate values of q_{u}, *i.e.*, $\bar{q}_{\text{u}} < q_{\text{u}} < \bar{\bar{q}}_{\text{u}}$, we have $0 = f'(u_{\text{M}}) = f_{\text{b}}'(u_{\text{M}}) + q_{\text{u}}$. To obtain a definition for all values of q_{u} we define the restriction $\tilde{f}_{\text{b}} = f_{\text{b}}|_{(u_{\text{infl}}, u_{\max})}$. Then $\tilde{f}_{\text{b}}'$ is increasing and we define

$$u_{\text{M}} = \begin{cases} u_{\max} , & 0 < q_{\text{u}} \le \bar{q}_{\text{u}} , \\ (\tilde{f}_{\text{b}}')^{-1}(-q_{\text{u}}) , & \bar{q}_{\text{u}} < q_{\text{u}} < \bar{\bar{q}}_{\text{u}} , \\ u_{\text{infl}} , & q_{\text{u}} \ge \bar{\bar{q}}_{\text{u}} . \end{cases}$$

Given u_{M} we define u_{m} as the unique concentration satisfying

$$f(u_{\text{m}}) = f(u_{\text{M}}) , \quad 0 < u_{\text{m}} \le u_{\text{infl}} ,$$

see Figure 2 (right).

2.3. The mathematical model

The mathematical model is described in [42] and we outline it only briefly here. We extend the space variable to the whole real line by assuming that the particles outside the settler have the same speed as the liquid. The total flux function is defined as

$$F(u,x) = \begin{cases} -q_{\text{e}} u , & x < -H , \\ g(u) = f_{\text{b}}(u) - q_{\text{e}} u , & -H < x < 0 , \\ f(u) = f_{\text{b}}(u) + q_{\text{u}} u , & 0 < x < D , \\ q_{\text{u}} u , & x > D . \end{cases} \tag{2}$$

The conservation law (preservation of mass) can be written as

$$u_t + (F(u,x))_x = s(t)\delta(x) , \tag{3}$$

where δ is the Dirac measure and the source function

$$s(t) = \frac{Q_{\text{f}}}{A} u_{\text{f}}(t) = \frac{Q_{\text{u}} + Q_{\text{e}}}{A} u_{\text{f}}(t) = (q_{\text{u}} + q_{\text{e}}) u_{\text{f}}(t) \tag{4}$$

describes the feed flux, *i.e.*, the mass per unit time and unit settler area entering the settler. Equation (3) should be interpreted in the weak sense. It reduces to

$$u_t + g(u)_x = 0 \qquad \text{in the clarification zone ,}$$

$$u_t + f(u)_x = 0 \qquad \text{in the thickening zone ,}$$

and to linear equations in the regions outside the settler. Within each zone the method of characteristics can be used together with the jump condition and the entropy condition by Oleinik [33] to construct solutions. At boundary discontinuities the situation is more complicated. At the feed inlet, $x = 0$, the jump condition is

$$f\left(u^+(t)\right) = g\left(u^-(t)\right) + s(t) , \tag{5}$$

where $u^{\pm}(t)$ are the boundary concentrations at $x = 0\pm$. This equation is not sufficient to determine the two boundary concentrations uniquely. Analogously, the jump conditions at the effluent and underflow levels are

$$\begin{aligned} g\left(u^H(t)\right) &= -q_e u_e(t) \qquad \text{at } x = -H\ , \\ f\left(u^D(t)\right) &= q_u u_u(t) \qquad \text{at } x = D\ , \end{aligned} \tag{6}$$

where u^H and u^D are the boundary concentrations within the settler at the top and bottom, respectively. This type of non-uniqueness originating from the discontinuities in $F(u,\cdot)$ is resolved by the entropy condition introduced in [41], which is a generalization of Oleinik's entropy condition. With this condition unique solutions for the whole settler including the prediction of the outlet concentrations can be constructed, see [42, 44]. Some regularity assumptions on piecewise smoothness and piecewise monotonicity of the solution at the boundaries are required. However, these cause no restrictions in the present application.

3. The steady states

3.1. THE SOLIDS-FLUX THEORY

The classical solids-flux theory is described and commented upon in several papers, *e.g.*, Jernqvist [9–11], Ozinsky *et al.* [29], and Keinath [22] and Chancelier *et al.* [43]. Examples of graphical constructions are shown in Figure 3. The intersection of the 'operating line' $y = s - q_u u$ and the 'effluent line' $y = q_e u$ defines the 'state point'. This occurs at the concentration u_f because of (4). If, for intermediate feed concentrations, the operating line cuts the batch-flux curve two or three times, then it is known that the settler will become overloaded. This is called thickening failure and occurs thus for $s - q_u u_M > f_b(u_M) \Leftrightarrow s > f(u_M)$, where $f(u_M)$ is called the limiting flux, *cf.* Figure 2 (right). Several other physically interesting cases of steady-state situations are also described in the literature, however, not all.

The concept of state point is slightly misleading, because it does not describe the state of the settler at the present time. It corresponds to the asymptotic state that is reached after a long or infinite time, provided the input variables are constant. Therefore, we do not adopt this terminology. Although the solids-flux theory only deals with steady-state conditions, conclusions are sometimes drawn on transient behaviours, in particular, at overflow situations. This means that assumptions on the concentrations (the solution of the conservation law) are made, which may not be correct. In waste-water treatment, where large sedimentation tanks are used partly as buffers of mass of biological sludge, a transient behaviour with $s \neq q_u u_u$ (feed flux $\neq$ underflow flux) may be present and wanted for several hours. Hence, the settler is not in steady state and the solids-flux theory is not sufficient to describe such a situation. If the

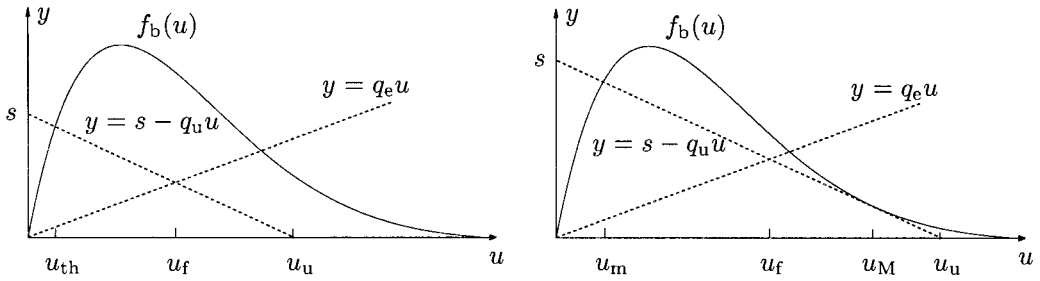

Figure 3. Examples of the classical graphical construction. Left: Underloaded conditions. u_{th} is the constant concentration in the thickening zone. Right: Critical conditions. The operating line is tangent to the batch flux curve at $(u_M, f_b(u_M))$. There is a discontinuity between u_m and u_M in the thickening zone.

operating line moves above the whole curve, or intersects it only once at a high concentration, the situation is called clarification failure (Laquidara and Keinath [21]), which is referred to as a transient situation. This will be analysed in a subsequent paper [51].

3.2. Operating charts for steady states and graphical constructions

3.2.1. *Preliminaries*

By using the knowledge of the solutions of (3), see [42, 47], the limitations of the solids-flux theory can be overcome. All steady-state solutions have been presented in these papers as a mere result of investigating the existence and uniqueness of solutions (with a constant and a varying cross-sectional area, respectively). For the control of the process it is vital to have a simpler way of presenting these solutions. In this section we show how all steady-state solutions can be classified in terms of only one table and an operating chart giving a much better overview. Moreover, we show how the concentrations of a steady-state solution can be obtained uniquely by a graphical construction, given the feed concentration and feed flux.

In the two classical concentration-flux diagrams shown in Figure 3 the concentrations in the thickening zone and the underflow concentration can be obtained along the operating line. However, the flux in the thickening zone and at the lower outlet has the constant value s. Accordingly, it is more natural to have the operating line horizontal in a concentration-flux diagram. Because of this and the jump condition (5) we draw the graphs of $f(u)$ and $g(u)+s$ in the same concentration-flux diagram, which we call an *operating chart*, see Figure 4. This means that we add the bulk flux $q_{\mathrm{u}}u$ to the graphs of $f_{\mathrm{b}}(u)$ and the straight lines in Figure 3. Then the previous operating line becomes horizontal at the flux value s that is present at every depth in the thickening zone for an underloaded or critically loaded settler. The previous overflow line becomes $y = (q_{\mathrm{u}} + q_{\mathrm{e}})u$, which we call the *feed line*, *cf.* (4). Note that u_{f} is the unique intersection of the graphs of $f(u)$ and $g(u)+s$ as well as of the effluent line $y = s - q_{\mathrm{e}}u$ and the underflow line $y = q_{\mathrm{u}}u$. The feed variables define the *feed point*

$$(u_{\mathrm{f}}, s) \in \Omega \equiv \left\{(u, y) : 0 < u \leq u_{\max},\ y > 0\right\}.$$

Note that when considering steady-state solutions we assume that $u_{\mathrm{f}} > 0$. Otherwise only the trivial zero solution applies. Since we also assume that $Q_{\mathrm{f}} > 0$ ($Q_{\mathrm{f}} = 0$ corresponds to batch sedimentation), only $s = Q_{\mathrm{f}}u_{\mathrm{f}}/A > 0$ is valid.

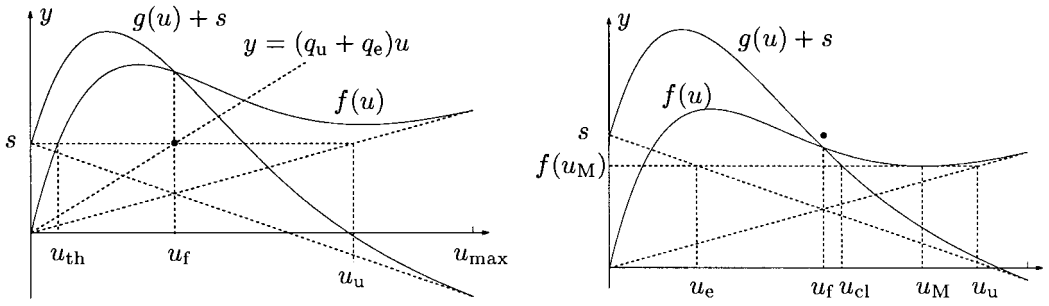

Figure 4. Examples of graphical constructions for obtaining steady-state concentrations. Left: Underloaded conditions, *cf.* Figure 3 (left). Right: Overloaded conditions with a nonzero effluent concentration, the constant concentration u_{cl} in the clarification zone and $u_{\mathrm{th}} = u_{\mathrm{M}}$ in the thickening zone.

For overloaded situations the classical construction with its operating line does not give any information on the steady-state concentrations. Figure 4 (right) shows how the steady-state concentrations can be obtained. We comment on this in the context of Figure 6.

3.2.2. *The steady-state chart*
In order to describe all steady-state solutions by the aim of an operating chart and to justify the constructions in Figure 4 we need two key fluxes. A generalized definition of the *limiting flux* is given by Chancelier *et al.* [40]:

$$f_{\lim}(u) = \min_{u \le \alpha \le u_{\max}} f(\alpha) = \begin{cases} f(u)\,, & u \in [0, u_{\mathrm{m}}] \cup [u_{\mathrm{M}}, u_{\max}]\,, \\ f(u_{\mathrm{M}})\,, & u \in (u_{\mathrm{m}}, u_{\mathrm{M}})\,, \end{cases} \tag{7}$$

see Figure 5. We define the *excess flux* as

$$\mathcal{E}(u_{\mathrm{f}}, s) = s - f_{\lim}(u_{\mathrm{f}})$$

and the following subsets of Ω:

$$\begin{aligned}
\mathcal{U}_1 &= \{(u, y) : 0 < q_{\mathrm{u}} u \le y < \min\left(f(u_{\mathrm{M}}), f(u)\right)\}\,, \\
\mathcal{U}_2 &= \{(u, y) : u_{\mathrm{M}} < u \le u_{\max},\ f(u_{\mathrm{M}}) < y < f(u),\ y \ge q_{\mathrm{u}} u\}\,, \\
\ell_1 &= \{(u, f(u)) : 0 < u < u_{\mathrm{m}}\}\,, \\
p &= (u_{\mathrm{m}}, f(u_{\mathrm{m}}))\,, \\
\ell_2 &= \{(u, f(u_{\mathrm{M}})) : u_{\mathrm{m}} < u \le u_{\mathrm{M}}\}\,, \\
\ell_3 &= \left\{(u, f(u_{\mathrm{M}})) : u_{\mathrm{M}} < u \le \frac{f(u_{\mathrm{M}})}{q_{\mathrm{u}}}\right\}\,, \\
\ell_4 &= \{(u, f(u)) : u_{\mathrm{M}} < u \le u_{\max}\}\,, \\
\ell_5 &= \{(u_{\mathrm{m}}, y) : y > f(u_{\mathrm{M}})\}\,, \\
\mathcal{O}_1 &= \{(u, y) : 0 < u < u_{\mathrm{m}},\ y > f(u)\}\,, \\
\mathcal{O}_2 &= \{(u, y) : u_{\mathrm{m}} < u \le u_{\mathrm{M}},\ y > f(u_{\mathrm{M}})\}\,, \\
\mathcal{O}_3 &= \{(u, y) : u_{\mathrm{M}} < u \le u_{\max},\ y > f(u)\}\,.
\end{aligned}$$

THEOREM 1. *With respect to the location of the feed point* $(u_{\mathrm{f}}, s) \in \Omega$ *all steady states of the settler are described by the* steady-state chart *shown in Figure 5 and the accompanying Table 1. For each* $(u_{\mathrm{f}}, s) \in \mathcal{U}_1 \cup \mathcal{U}_2 \cup \mathcal{O}_1 \cup \mathcal{O}_2 \cup \mathcal{O}_3$ *there exists a unique steady-state solution. If* $(u_{\mathrm{f}}, s) \in \bigcup_{i=1}^{5} \ell_i$ *there exists a steady-state solution, which is uniquely determined except for the location of a discontinuity.*

The proof consists in rearranging all steady-state solutions as presented in [42, 47]. The last two statements are commented upon in the context of the mass of the settler, see (9) and (10). Note that the feed point always lies on or above the line $y = q_{\mathrm{u}} u$, because $s = (q_{\mathrm{u}} + q_{\mathrm{e}}) u_{\mathrm{f}} \ge q_{\mathrm{u}} u_{\mathrm{f}}$. It should be noted that in Table 1 u_{m} and u_{M} each has the same value in the whole table, since Q_{u} (and q_{u}) has a fixed value independently of the feed point. However, the positive zero u_{z} of g varies with the feed point, because (4) implies that

$$g(u) = f_{\mathrm{b}}(u) - q_{\mathrm{e}} u = f_{\mathrm{b}}(u) - \left(\frac{s}{u_{\mathrm{f}}} - q_{\mathrm{u}}\right) u\,.$$

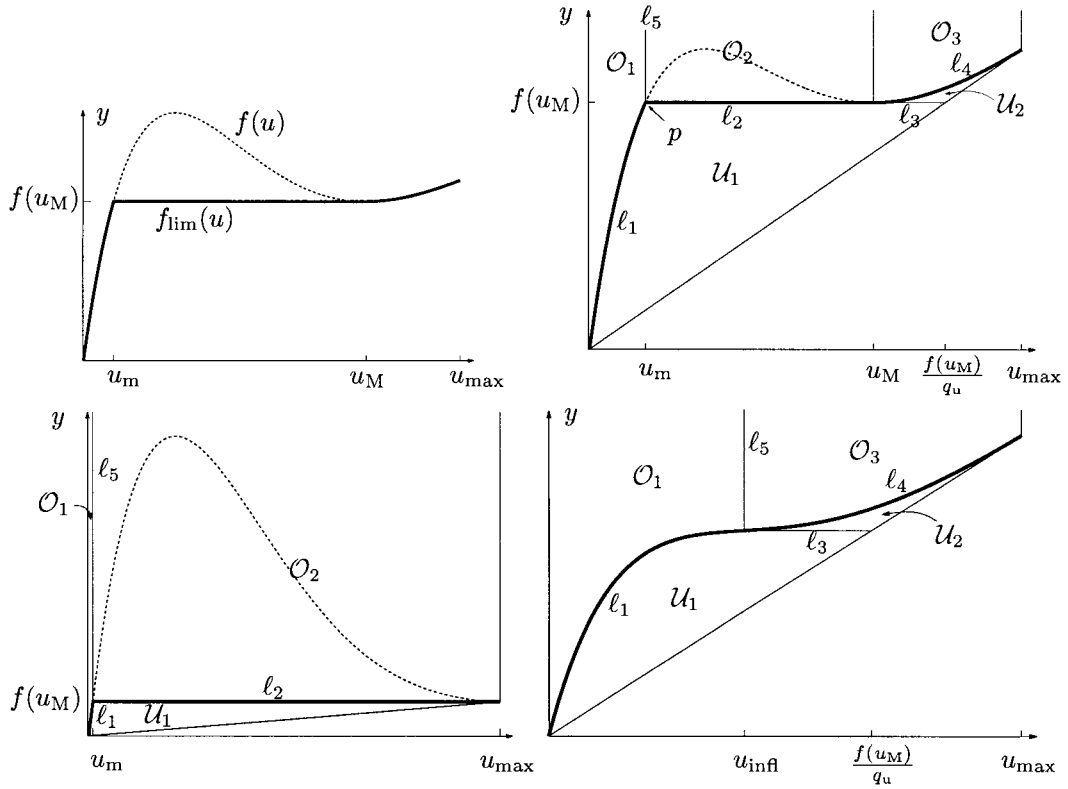

Figure 5. The limiting flux (upper left). The steady-state chart in the cases $\bar{q}_\mathrm{u} < q_\mathrm{u} < \bar{\bar{q}}_\mathrm{u}$ (upper right), $0 < q_\mathrm{u} \le \bar{q}_\mathrm{u}$ (lower left) and $q_\mathrm{u} > \bar{\bar{q}}_\mathrm{u}$ (lower right).

Note also that some regions become empty for values of q_u outside the interval $(\bar{q}_\mathrm{u}, \bar{\bar{q}}_\mathrm{u})$. Furthermore, if $q_\mathrm{e} = 0$ then there is no effluent flow and u_e is not defined. Recall that we have required $q_\mathrm{u} > 0$.

3.2.3. *Consequences*

There are several interesting consequences of Theorem 1. Firstly, it is natural to say that the settler is *underloaded* if $\mathcal{E}(u_\mathrm{f}, s) < 0$, *overloaded* if $\mathcal{E} > 0$ and *critically loaded* if $\mathcal{E} = 0$ (*cf.* Figure 6). Let f_thick denote the flux in the thickening zone in steady state. From Table 1 it is possible to extract the following explicit formulae.

COROLLARY 1. *Given a feed point* $(u_\mathrm{f}, s) \in \Omega$ *the following holds in steady state:*

$$\begin{aligned} f_\mathrm{thick}(u_\mathrm{f}, s) &= \min\,(s,\, f_\mathrm{lim}(u_\mathrm{f}))\ , & u_\mathrm{u}(u_\mathrm{f}, s) &= \frac{A f_\mathrm{thick}(u_\mathrm{f}, s)}{Q_\mathrm{u}}\ , \\ Q_\mathrm{e}(u_\mathrm{f}, s) &= \frac{As}{u_\mathrm{f}} - Q_\mathrm{u}\ , & u_\mathrm{e}(u_\mathrm{f}, s) &= \frac{A \max\,(0, \mathcal{E}(u_\mathrm{f}, s))}{Q_\mathrm{e}} \quad (Q_\mathrm{e} > 0)\ . \end{aligned} \tag{8}$$

Note that u_e is not defined if $Q_\mathrm{e} = 0$. The property of f_thick motivates the definition of the limiting flux, see Figure 6, which shows the common cases of underloaded and overloaded settler for intermediate feed concentrations.

Now we can generalize the concept of *operating line* to be the horizontal line $y = f_\mathrm{thick}(u_\mathrm{f}, s)$. For example, in both Figures 4 and 6 the operating lines are $y = s$ (left

Table 1. The steady states of the settler. If the concentration in the clarification zone is constant, it is denoted by u_{cl}. The notation with braces means either that the concentration is either zero or u_z in the whole clarification zone, or there is a discontinuity within the zone with the concentration zero above and u_z below. (In some of the cases only two of these three alternatives are actually possible, but we refrain from distinguishing such subtle subcases.) An analogous notation is used for the thickening zone.

Region in s-s chart	Excess flux	Effluent conc. u_e	Underflow conc. u_u	Solution in clarification zone u_{cl}	Solution in thicken. zone u_{th}
$\mathcal{U}_1$	$\mathcal{E} < 0$	0	$\dfrac{s}{q_u}$	$u_{cl} = 0$	$u_{th} < u_m$ $s = f(u_{th})$
$\mathcal{U}_2$					$u_M < u_{th} < u_f$ $s = f(u_{th})$
ℓ_3			$\dfrac{f(u_M)}{q_u}$		$u_{th} = \begin{cases} u_m \\ u_M \end{cases}$
ℓ_2	$\mathcal{E} = 0$			$u_{cl} = \begin{cases} 0 \\ u_z \end{cases}$ $u_m < u_z \le u_M$	$u_{th} = u_M$
p				$u_{cl} = \begin{cases} 0 \\ u_z = u_f = u_m \end{cases}$	$u_{th} = \begin{cases} u_m \\ u_M \end{cases}$
ℓ_1			$\dfrac{f(u_f)}{q_u}$	$u_{cl} = \begin{cases} 0 \\ u_z = u_f < u_m \end{cases}$	$u_{th} = u_f < u_m$
ℓ_4				$u_{cl} = \begin{cases} 0 \\ u_z = u_f > u_M \end{cases}$	$u_{th} = u_f > u_M$
$\mathcal{O}_1$	$\mathcal{E} > 0$	$\dfrac{s - f(u_f)}{q_e}$		$u_z < u_{cl} = u_f < u_m$	$u_{th} = u_f$
ℓ_5		$\dfrac{s - f(u_M)}{q_e}$	$\dfrac{f(u_M)}{q_u}$	$u_z < u_{cl} = u_f = u_m$	$u_{th} = \begin{cases} u_m \\ u_M \end{cases}$
$\mathcal{O}_2$				$u_{cl} > \max(u_f, u_z)$ $g(u_{cl}) + s = f(u_M)$	$u_{th} = u_M$
$\mathcal{O}_3$		$\dfrac{s - f(u_f)}{q_e}$	$\dfrac{f(u_f)}{q_u}$	$u_{cl} = u_f > u_z$	$u_{th} = u_f > u_M$

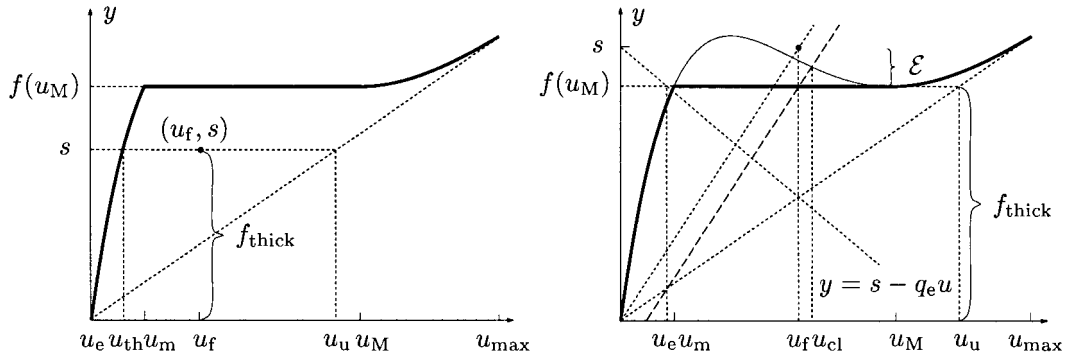

Figure 6. Left: Underloaded settler; $(u_f, s) \in \mathcal{U}_1$. The thickening zone can handle all the feed flux; $f_{\text{thick}} = s$. Right: Overloaded settler; $(u_f, s) \in \mathcal{O}_2$. The upward flux in the clarification zone is equal to the excess flux; $s - f_{\text{thick}} = \mathcal{E}$. A graphical construction of all concentrations without using g is demonstrated; $u_{\text{th}} = u_M$.

charts) and $y = f(u_M)$ (right charts). It is time to comment on the graphical way of obtaining u_e and u_{cl} in these two figures, particularly the right charts, in which $(u_f, s) \in \mathcal{O}_2$. Table 1 gives that the concentration in the clarification zone is constant and given by $f(u_M) = g(u_{cl}) + s$, hence it is obtained as the intersection of the operating line $y = f(u_M)$ and the graph of $g(\cdot)+s$ (Figure 4, right). The conservation of mass at the effluent at $x = -H$ is $g(u_{cl}) = -q_e u_e$, see (6). Hence, $f(u_M) = s + g(u_{cl}) = s - q_e u_e$, which explains that u_e is obtained as the intersection of the operating line and the effluent line $y = s - q_e u$. These concentrations can also be obtained without the use of g and the effluent line. Draw the line $y = f(u_M)+(q_u+q_e)(u-u_f)$ (long dashes in Figure 6 (right)), which is parallel to the feed line and passes through the point $(u_f, f(u_M))$. u_{cl} is obtained from the intersection of this line and the graph of f. This can be seen from the definition of g and (4):

$$f(u_M) = g(u_{cl}) + s = f_b(u_{cl}) - q_e u_{cl} + (q_u + q_e)u_f =$$
$$= f_b(u_{cl}) + q_u u_{cl} - (q_u + q_e)(u_{cl} - u_f) = f(u_{cl}) - (q_u + q_e)(u_{cl} - u_f)$$
$$\iff \quad f(u_M) + (q_u + q_e)(u_{cl} - u_f) = f(u_{cl}) \, .$$

Furthermore, u_e is the intersection of the latter drawn line and the underflow line $y = q_u u$, since

$$f(u_M) = g(u_{cl}) + s = -q_e u_e + (q_u + q_e)u_f = -(q_u + q_e)(u_e - u_f) + q_u u_e \quad \iff$$
$$f(u_M) + (q_u + q_e)(u_e - u_f) = q_u u_e \, .$$

The concentration profile within the settler in steady state is always non-decreasing with depth and piecewise constant with at most two discontinuities and at most one discontinuity in each of the two zones, see Table 1. The only possibility for a steady-state solution having discontinuities both in the clarification and thickening zone is for $(u_f, s) = p$.

For $(u_f, s) \in \ell_2 \cup \ell_3$ there is a possible discontinuity in the thickening zone, which we call the *sludge blanket* using the terminology from waste-water treatment. Its existence is possible only if $s = f(u_M)$ and it can be located at any depth in the thickening zone. The concentration above and below it is u_m and u_M, respectively, see Table 1. Then the total mass satisfies $m < ADu_M$. If $m = ADu_M$ and $(u_f, s) \in \ell_2 \cup \ell_3$, then the sludge blanket is located at the feed level with zero concentration above and u_M below. If $m > ADu_M$, then there is a discontinuity in the clarification zone between zero and u_z. We may say that the sludge blanket is forced above the feed level. This may occur for $(u_f, s) \in \ell_1 \cup \ell_2 \cup \ell_4$.

For $(u_{\rm f}, s) \in \bigcup_{i=1}^{5} \ell_i$ at most one discontinuity (sludge blanket) is possible within the clarification or thickening zone. Let $x = x_{\rm sb}$ be its location. From Table 1 we get that the mass in the settler is

$$\begin{aligned}
\ell_1 \cup \ell_4 : \quad & m = A(D - x_{\rm sb})u_{\rm f} \,, \quad -H \le x_{\rm sb} \le 0 \,, \\
\ell_2 : \quad & m = \begin{cases} A(-x_{\rm sb}u_{\rm z} + Du_{\rm M}) \,, & -H \le x_{\rm sb} < 0 \,, \\ A\left(x_{\rm sb}u_{\rm m} + (D - x_{\rm sb})\, u_{\rm M}\right) \,, & 0 \le x_{\rm sb} \le D \,, \end{cases} \\
\ell_3 : \quad & m = A\left(x_{\rm sb}u_{\rm m} + (D - x_{\rm sb})u_{\rm M}\right) \,, \quad 0 \le x_{\rm sb} \le D \,, \\
\ell_5 : \quad & m = A\left((H + x_{\rm sb})u_{\rm m} + (D - x_{\rm sb})u_{\rm M}\right) \,, \quad 0 \le x_{\rm sb} \le D \,.
\end{aligned} \tag{9}$$

For each of these regions m is a decreasing (and continuous) function of $x_{\rm sb}$. Hence, for given $(u_{\rm f}, s) \in \bigcup_{i=1}^{5} \ell_i$ there exists a steady-state solution, which is uniquely determined by a given total mass or, equivalently, the location $x_{\rm sb}$ of the sludge blanket.

For $(u_{\rm f}, s) \in \mathcal{U}_1 \cup \mathcal{U}_2 \cup \mathcal{O}_1 \cup \mathcal{O}_2 \cup \mathcal{O}_3$ there exists a unique steady-state solution and the mass in the different regions can be extracted from Table 1:

$$m(u_{\rm f}, s) = \begin{cases} ADu_{\rm th}(s) \,, & (u_{\rm f}, s) \in \mathcal{U}_1 \cup \mathcal{U}_2 \,, \\ A(H + D)u_{\rm f} \,, & (u_{\rm f}, s) \in \mathcal{O}_1 \cup \mathcal{O}_3 \,, \\ A\left(Hu_{\rm cl}(u_{\rm f}, s) + Du_{\rm M}\right) \,, & (u_{\rm f}, s) \in \mathcal{O}_2 \,. \end{cases} \tag{10}$$

This information can be shown in an operating chart, see Figure 7.

A critically loaded settler becomes over/underloaded in the new steady state if $Q_{\rm f}$, and thereby s, increases/decreases and $u_{\rm f}$ is fixed – the feed point moves vertically up/down. What happens if $Q_{\rm f}$ is fixed and the feed concentration varies? Then the feed point moves along the feed line $y = (q_{\rm u} + q_{\rm e})u = \frac{Q_{\rm f}}{A}u$ because of (4), see Figure 8. The statement of the proposition below is natural, however, it may not be true for some feed points in ℓ_1 or ℓ_4 in the case $f_{\rm b}$ has more than one inflection point; *cf.* [52–54].

PROPOSTION 1. *Given a critically loaded settler with $u_{\rm f} \in (0, u_{\max}]$ and $f_{\rm b}$ satisfying (1). If the feed concentration changes to $u_{\rm f1} \in (0, u_{\max}]$ and $Q_{\rm f}$ is fixed, then*

$$u_{\rm f1} - u_{\rm f} < 0 \ (> 0) \quad \Longrightarrow \quad \textit{the settler will become underloaded } (\textit{overloaded}) \,.$$

Graphically, the proposition says that the feed line $y = (q_{\rm u} + q_{\rm e})u$ intersects the graph of $f_{\rm lim}(u)$ only at the point $(u_{\rm f}, f_{\rm lim}(u_{\rm f}))$ except for the origin, see Figure 8. We omit the proof, which is a minor modification of the proof of the second statement of Lemma 1 in the Appendix.

4. On the control of the steady states

4.1. System purposes, control criteria and objectives

The aims of the settler may vary depending on in what industrial process it is involved. At least in waste-water treatment the main *purposes* of the settler are the following. It should

1. produce a low effluent concentration.
2. produce a high underflow concentration.
3. work as a buffer of mass and be insensitive to small variations in the feed variables.

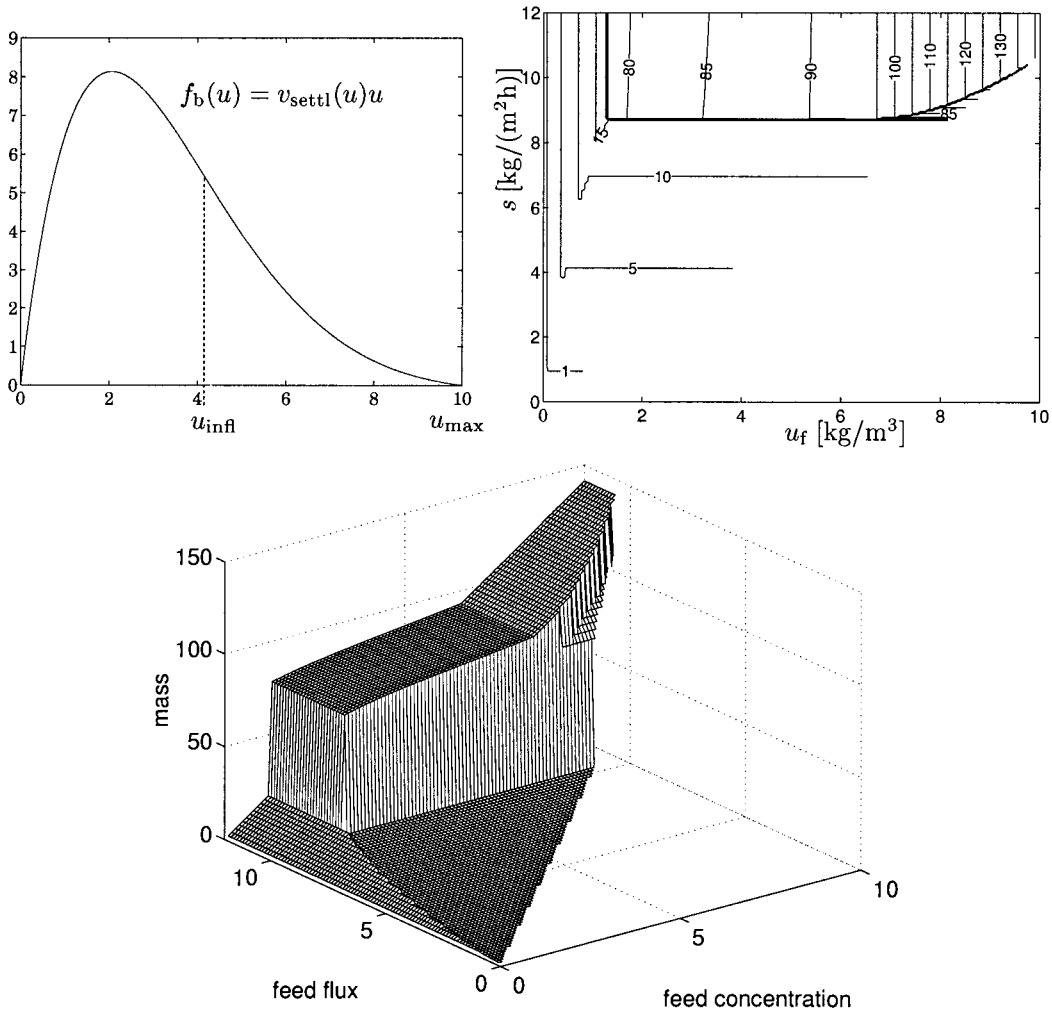

Figure 7. Upper left: Batch-settling flux used for the numerical results in this paper: $f_b(u) = 10u\left((1 - 0{\cdot}64u/u_{max})^{6{\cdot}55} - 0{\cdot}36^{6{\cdot}55}\right)$ [kg/(m^{2}h)]. Upper right and lower: Contours and graph of $m(u_f, s)$ [tonnes] given by (10). The numerical values used are $H = 1$ m, $D = 4$ m, $A = \pi(30\text{ m})^2 = 2827$ m^2 and $Q_u = 3000$ m^3/h.

These purposes cannot be controlled independently. Besides fulfilling the main purposes a control strategy should be able to utilize the capacity of the settler, *i.e.*, a control strategy should

4. maximize the capacity of the thickening zone.
5. maximize the effluent flow.

The above purposes have various implicit economic aspects. Such aspects are also related to the treatment before and after the continuous-sedimentation process. These issues, however, are beyond the scope of the present study. One aim of this paper is to present quantitative descriptions of the steady states in order to facilitate the formation of control criteria and objectives with respect to the five purposes above. In order to specify and suggest such things we need to know how the characteristic concentrations, fluxes and the steady-state regions of the operating chart depend on the control variable Q_u. Therefore, we define

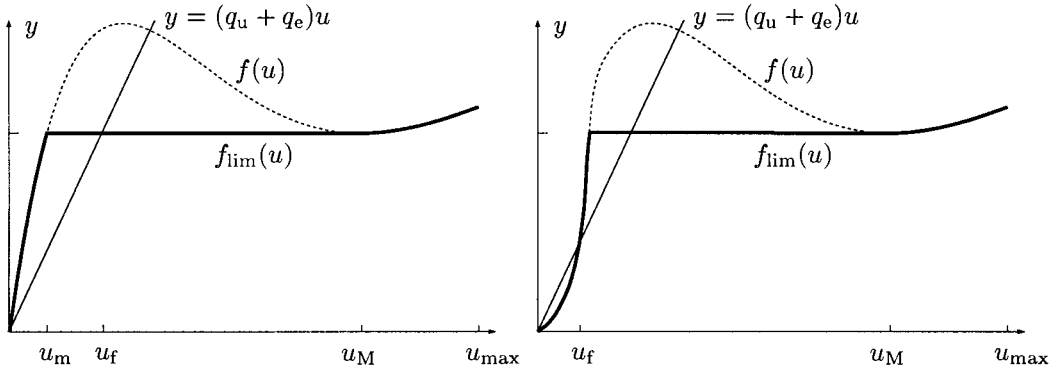

Figure 8. Left: Illustration to Proposition 1. Right: A flux curve with more than one inflection point. Given the location of $(u_f, f_{lim}(u_f))$ the contrast to Proposition 1 holds, *e.g.*, a decrease in u_f will result in an overloaded settler.

$$\bar{Q}_u = A\bar{q}_u\,, \qquad \overline{\overline{Q}}_u = A\bar{\bar{q}}_u$$

and from now on write out the dependence on the feed point and Q_u, for example,

$$Q_e(u_f, s, Q_u) = \frac{As}{u_f} - Q_u\,, \tag{11}$$

$u_M(Q_u)$ (see Figure 9), $f(u, Q_u)$, $\mathcal{E}(u_f, s, Q_u)$, $f_{thick}(u_f, s, Q_u)$, $\ell_1(Q_u)$, etc. These functions are continuous and differentiable almost everywhere. Their monotonicity properties with respect to Q_u are given in Lemma 2 in the Appendix. With references to these monotonicity properties, the steady-state formulae (8) and the purposes of the settler given above we consider the following *control criteria,* which are formulated in terms of the output variables on the left-hand side and the feed point and the control variable on the right-hand side (disregarding the point $p(Q_u)$):

1.	$u_e = 0$	$\Longleftrightarrow$	$\mathcal{E}(u_f, s, Q_u) \le 0$
2.	u_u is maximized	$\Longleftrightarrow$	Q_u is minimized
3.	$u_{cl} = 0$ and there is a discontinuity at $x_{sb} \in (0, D)$ in the thickening zone	$\Longleftrightarrow$	$(u_f, s) \in \ell_2(Q_u) \cup \ell_3(Q_u)$ and $u_m(Q_u) < m(x_{sb}, Q_u)/(AD) < u_M(Q_u)$
4.	f_{thick} is maximized	$\Longleftrightarrow$	$\mathcal{E}(u_f, s, Q_u) \ge 0$
5.	Q_e is maximized	$\Longleftrightarrow$	Q_u is minimized

We say that the settler is in *optimal operation* (in steady state) if criterion 3 is satisfied. The right implication follows from Table 1 and the left one from (9). This means that Figure 9 can be used as an operating chart for the linear relationship (*cf.* (9)) between $m(x_{sb}, Q_u)$ and x_{sb}. For a fixed Q_u the vertical line between $(Q_u, u_M(Q_u))$ and $(Q_u, u_m(Q_u))$ (there are two dashed such in Figure 9) represents the depth of the thickening zone, with $x = 0$ at $(Q_u, u_M(Q_u))$ and $x = D$ at $(Q_u, u_m(Q_u))$. Along this line, from top to bottom, the possible values of $m(x_{sb}, Q_u)/(AD)$ can be read on the u-axis, and these values increase linearly as x_{sb} increases from 0 to D. For example, in the middle of the interval the mass is $m = AD(u_m + u_M)/2$ corresponding to $x_{sb} = D/2$, *i.e.*, a sludge blanket in the middle of the thickening zone. We also note that criterion 3 implies that $Q_u < \overline{\overline{Q}}_u$, because otherwise $u_M(Q_u) = u_m(Q_u) = u_{infl}$, which is a contradiction. During dynamic behaviour the total mass depends

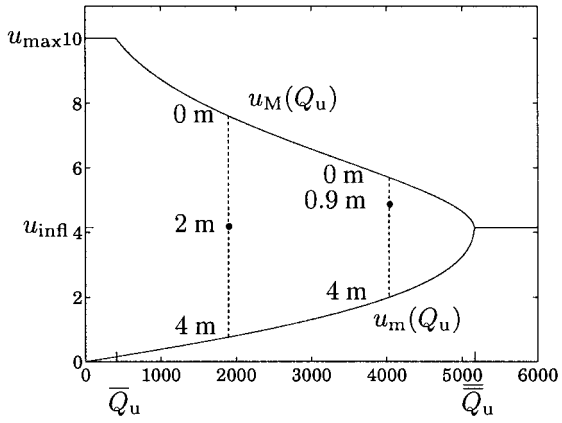

Figure 9. Graphs of $u_M(Q_u)$ and $u_m(Q_u)$ (solid lines), which coincide for $Q_u \geq \overline{\overline{Q}}_u = 5168\ \mathrm{m}^3/\mathrm{h}$. The figure also serves as an operating chart for optimal operation showing the relationship between $m(x_{sb}, Q_u)/(AD)$ (read on the u-axis) and the depth of the sludge blanket x_{sb}. The two points on the dashed lines correspond to the initial and final steady states, respectively, of the example in Section 5, where $D = 4$ m. Each dashed line represents the depth of the thickening zone.

on the solution, which also depends on when a control action is performed. This makes it difficult to obtain general control strategies beforehand for obtaining a specific sludge blanket depth, *cf.* the example in Section 5. Information on the transient behaviour will be given in a subsequent paper [51].

Control actions for fulfilling the other criteria can be performed at any time. Besides the given criteria there may be constraints that limit the possibilities of a control action, for example, an upper bound on the control variable because of a limited pump capacity. The control criteria may be weighted together differently in different applications. However, natural *control objectives* are:

- The settler is in optimal operation.
- $(u_f, s) \in p(Q_u) \cup \ell_2(Q_u) \cup \ell_3(Q_u)$.
- $\mathcal{E}(u_f, s, Q_u) = 0 \iff (u_f, s) \in \ell_1(Q_u) \cup p(Q_u) \cup \ell_2(Q_u) \cup \ell_4(Q_u)$.
- $\mathcal{E}(u_f, s, Q_u) \leq 0$ with $u_u(u_f, s, Q_u)$ and $Q_e(u_f, s, Q_u)$ lying in prescribed intervals.

Only the last objective concerns control criteria 2 and 5. The first objective is discussed above and information on the possibility of fulfilling the others are given in the next section.

4.2. Operating charts for control

For the control objectives stated above it is vital to find a value of the control variable Q_u such that $\mathcal{E}(u_f, s, Q_u) = 0 \Leftrightarrow s = f_{lim}(u_f, Q_u)$. Guided by the graphs of $f_{lim}(\cdot, Q_u)$ shown in Figure 10 (left) we define the regions in the operating chart:

$$\Lambda_i = \bigcup_{Q_u > 0} \ell_i(Q_u)\,, \quad i = 1, \ldots, 4\,,$$
$$P = P_1 \cup P_2\,, \quad \text{where} \quad P_1 = \bigcup_{0 < Q_u \leq \bar{\bar{Q}}_u} p(Q_u)\,, \quad P_2 = \bigcup_{Q_u > \bar{\bar{Q}}_u} p(Q_u)\,,$$

see Figure 10 (right).

THEOREM 2. *Given* $(u_f, s) \in \Omega = \{(u, y) : 0 < u \leq u_{max},\ y > 0\}$ *there exists a unique* $\tilde{Q}_u(u_f, s) > 0$ *such that* $\mathcal{E}(u_f, s, \tilde{Q}_u) = 0$ *and the following properties hold:*

$$(u_\mathrm{f}, s) \in \Lambda_i \quad \Longrightarrow \quad (u_\mathrm{f}, s) \in \ell_i(\tilde{Q}_\mathrm{u}) \,, \quad i = 1, 2, 4 \,,$$

$$(u_\mathrm{f}, s) \in P \quad \Longrightarrow \quad (u_\mathrm{f}, s) \in p(\tilde{Q}_\mathrm{u}) \,,$$

$$\frac{\partial \tilde{Q}_\mathrm{u}}{\partial u_\mathrm{f}} = \begin{cases} -\dfrac{A}{u_\mathrm{f}} \dfrac{\partial f}{\partial u}(u_\mathrm{f}, \tilde{Q}_\mathrm{u}) < 0 \,, & (u_\mathrm{f}, s) \notin \Lambda_2 \cup P_1 \,, \\ 0 \,, & (u_\mathrm{f}, s) \in \Lambda_2 \,, \end{cases}$$

$$\frac{\partial \tilde{Q}_\mathrm{u}}{\partial s} = \begin{cases} \dfrac{A}{u_\mathrm{f}} > 0 \,, & (u_\mathrm{f}, s) \notin \Lambda_2 \cup P_1 \,, \\ \dfrac{A}{u_\mathrm{M}(\tilde{Q}_\mathrm{u})} > 0 \,, & (u_\mathrm{f}, s) \in \Lambda_2 \,, \end{cases}$$

$\tilde{Q}_\mathrm{u}$ is a continuous function on Ω,

$$\mathcal{E}(u_\mathrm{f}, s, Q_\mathrm{u}) \le 0 \quad \Longleftrightarrow \quad Q_\mathrm{u} \ge \tilde{Q}_\mathrm{u}(u_\mathrm{f}, s) \,. \tag{12}$$

If $(u_\mathrm{f}, s) \in \Lambda_3$ *then there exists a unique* $Q_\mathrm{u} > 0$ *with* $(u_\mathrm{f}, s) \in \ell_3(Q_\mathrm{u})$.

(The proof can be found in the Appendix.) Equivalence (12) means that the settler is underloaded (or critically loaded) if and only if the value of the control variable is greater than (or equal to) the critical value $\tilde{Q}_\mathrm{u}$. If strict inequality applies the particles are flushed out through the underflow and there is no possibility for a sludge blanket within the thickening zone.

For each feed point the value $Q_\mathrm{u} = \tilde{Q}_\mathrm{u}(u_\mathrm{f}, s)$ is obtained by solving the non-linear equation $s = f_\mathrm{lim}(u_\mathrm{f}, Q_\mathrm{u})$. However, the contours of $\tilde{Q}_\mathrm{u}(u_\mathrm{f}, s)$ are easy to obtain since these are the family of graphs of $f_\mathrm{lim}(\cdot, Q_\mathrm{u})$, see Figure 10 (left), which thus constitutes an important operating chart.

Consider the last control objective stated in Section 4.1. For a given feed point in Ω the underflow concentration

$$u_\mathrm{u}(u_\mathrm{f}, s, Q_\mathrm{u}) = \frac{A f_\mathrm{thick}(u_\mathrm{f}, s, Q_\mathrm{u})}{Q_\mathrm{u}} = \begin{cases} \dfrac{As}{Q_\mathrm{u}} \,, & s \le f_\mathrm{lim}(u_\mathrm{f}, Q_\mathrm{u}) \\ \dfrac{A f_\mathrm{lim}(u_\mathrm{f}, Q_\mathrm{u})}{Q_\mathrm{u}} \,, & s > f_\mathrm{lim}(u_\mathrm{f}, Q_\mathrm{u}) \end{cases} \tag{13}$$

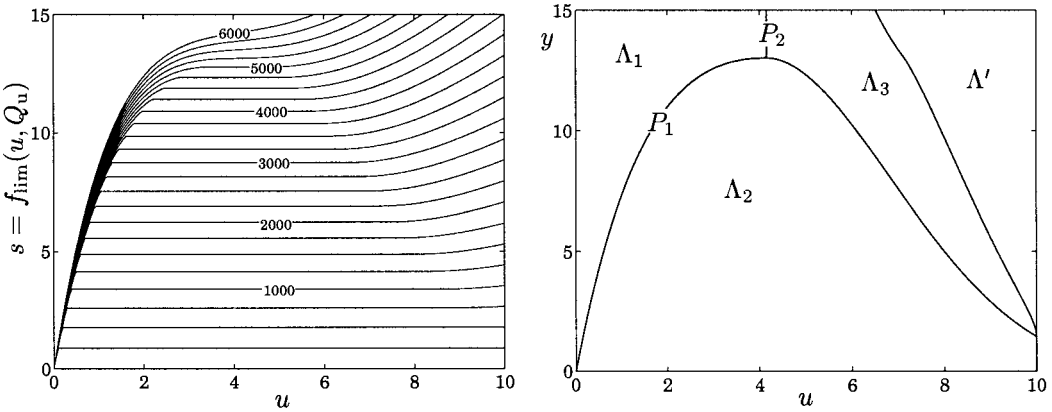

Figure 10. Operating charts for control of steady states. Left: Graphs of $f_\mathrm{lim}(\cdot, Q_\mathrm{u})$ for some values of Q_u. Right: The control chart. $\Lambda_4 = \Lambda_3 \cup \Lambda'$. Theorem 2 says that given a feed point in this chart there is a unique graph $f_\mathrm{lim}(\cdot, \tilde{Q}_\mathrm{u})$ that passes through the feed point. With the value $\tilde{Q}_\mathrm{u}$ the settler is critically loaded in steady state.

is a continuous function of Q_u, which is constant for small $Q_u > 0$ and then decreasing (at least for $Q_u \geq \bar{Q}_u$) by Lemma 2. Since f_{lim} is a continuous and increasing function of Q_u (Lemma 2), $f_{lim}(u_f, 0) = 0$ and $f_b(u_{max}) = 0$ it follows that

$$\lim_{Q_u \to 0+} u_u(u_f, s, Q_u) = \lim_{Q_u \to 0+} \frac{Af(u_{max}, Q_u)}{Q_u} = \lim_{Q_u \to 0+} \frac{Af_b(u_{max}) + Q_u u_{max}}{Q_u} = u_{max} ,$$

$$\inf_{0 < Q_u \leq Q_f} u_u(u_f, s, Q_u) = u_u(u_f, s, Q_f) = \frac{As}{Q_f} = u_f .$$

This, together with (A6), implies that any prescribed value on the underflow concentration in the interval $[u_f, u_{max})$ could be obtained by choosing an appropriate value of $Q_u > 0$. However, constraint (12), which ensures that the settler is not overloaded, reduces the maximum value of the underflow concentration:

$$u_f \leq u_u(u_f, s, Q_u) \leq u_u\left(u_f, s, \tilde{Q}_u(u_f, s)\right) = \frac{As}{\tilde{Q}_u(u_f, s)} \equiv \tilde{u}_u(u_f, s) .$$

Analogously, (12) implies an upper bound on the effluent volume flow because of (11):

$$0 \leq Q_e(u_f, s, Q_u) \leq \frac{As}{u_f} - \tilde{Q}_u(u_f, s) \equiv \tilde{Q}_e(u_f, s) .$$

Note that in the definitions of $\tilde{u}_u$ and $\tilde{Q}_e$ the relation $s = f_{lim}\left(u_f, s, \tilde{Q}_u(u_f, s)\right)$ holds. These functions are continuous on Ω and have the following properties (see the Appendix):

$$\frac{\partial \tilde{Q}_e}{\partial u_f} < 0 , \quad (u_f, s) \notin P_1 , \tag{14a}$$

$$\frac{\partial \tilde{Q}_e}{\partial s} \begin{cases} = 0 , & (u_f, s) \in \Lambda_1 \cup \text{closure}(\Lambda_4) , \\ > 0 , & (u_f, s) \in \text{interior}(\Lambda_2) , \end{cases} \tag{14b}$$

$$\tilde{Q}_e(u_f, s) \begin{cases} > 0 , & u_f < u_{max} , \\ = 0 , & u_f = u_{max} , \end{cases} \tag{14c}$$

$$\frac{\partial \tilde{u}_u}{\partial u_f} = -\frac{As}{\tilde{Q}_u^2} \frac{\partial \tilde{Q}_u}{\partial u_f} \begin{cases} > 0 , & (u_f, s) \notin \Lambda_2 \cup P_1 , \\ = 0 , & (u_f, s) \in \Lambda_2 , \end{cases} \tag{14d}$$

$$\frac{\partial \tilde{u}_u}{\partial s} \begin{cases} = 0 , & (u_f, s) \in \left(\Lambda_2 \cap \left\{(u, y) : y \leq \bar{q}_u u_{max}\right\}\right) \cup \left\{(u_{max}, y) : y > 0\right\} \equiv \Upsilon , \\ < 0 , & (u_f, s) \notin \Upsilon \cup P_1 , \end{cases} \tag{14e}$$

$$\tilde{u}_u(u_f, s) \begin{cases} = u_{max} , & (u_f, s) \in \Upsilon , \\ \in (0, u_{max}) , & (u_f, s) \notin \Upsilon . \end{cases} \tag{14f}$$

These properties provide further information in operating charts for control, see Figure 11. As a last interesting engineering concept we introduce the *thickening factor* $\theta = u_u/u_f$. The maximum capacity of the settler to thicken the feed concentration for a critically loaded settler is thus

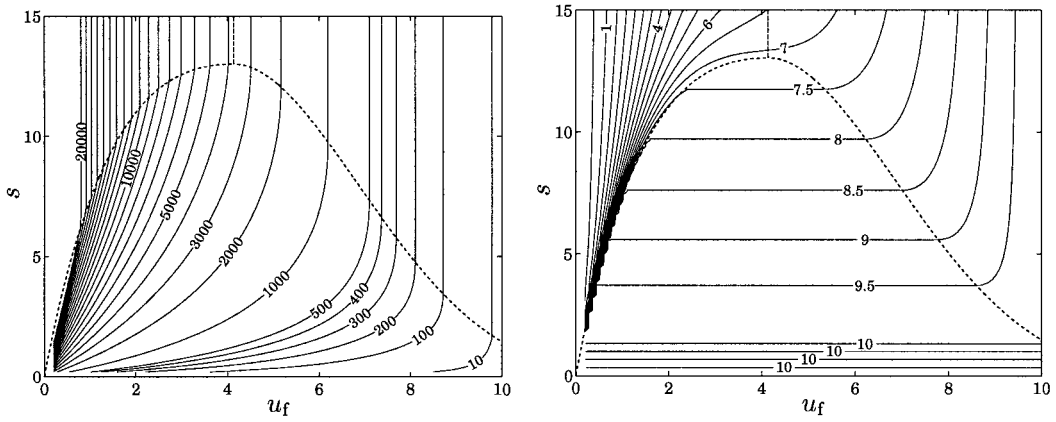

Figure 11. Operating charts with contours of the maximum values $\tilde{Q}_e(u_f, s)$ [m^3/h] (left) and $\tilde{u}_u(u_f, s)$ [kg/m^3] (right).

$$\tilde{\theta}(u_f, s) = \frac{\tilde{u}_u(u_f, s)}{u_f} = \frac{As}{\tilde{Q}_u(u_f, s)u_f} .$$

This is a continuous function on Ω and has the following monotonicity properties (see the Appendix):

$$\frac{\partial\tilde{\theta}}{\partial u_f} = \begin{cases} \dfrac{A^2 s}{\tilde{Q}_u^2 u_f^2} f_b'(u_f) , & (u_f, s) \notin \Lambda_2 \cup P_1 , \\ -\dfrac{As}{\tilde{Q}_u u_f^2} < 0 , & (u_f, s) \in \Lambda_2 , \end{cases} \tag{15a}$$

$$\frac{\partial\tilde{\theta}}{\partial s} = \frac{1}{u_f}\frac{\partial\tilde{u}_u}{\partial s} = \begin{cases} = 0 , & (u_f, s) \in \Upsilon , \\ < 0 , & (u_f, s) \notin \Upsilon \cup P_1 . \end{cases} \tag{15b}$$

Note the change of sign of $\partial\tilde{\theta}/\partial u_f$ in Λ_1 (Figure 12) at the concentration of the maximum of f_b (*cf.* Figure 7, upper left).

5. Example

Assume that the settler initially is in optimal operation with the feed point $(u_{f0}, s_0) \in \ell_2(Q_{u0})$, where $u_{f0} = 6$ kg/m^3, $s_0 = 6$ kg/(m^{2}h) and $Q_{u0} = 1908$ m^3/h, and that there is a sludge blanket in the middle of the thickening zone, *i.e.*, at the depth $x_{sb} = 2$ m. The feed concentration and flux increase linearly for $0 < t < 2$ h and for $t \geq 2$ h the feed point stays at $(u_f, s) = (7, 11) \in \Lambda_3$, see Figure 13. At $t = 2{\cdot}5$ h the control variable is increased by a step to $Q_u = 4045$ m^3/h, which implies that $(u_f, s) = (7, 11) \in \ell_3(Q_u)$ (*cf.* Theorem 2, last row). A numerical simulation is shown in Figure 14. The numerical algorithm presented in [55] is used. Note how a part of the fed mass is conveyed up into the clarification zone and that the settler would be overloaded unless the control variable were changed. As the control variable makes a step increase at $t = 2{\cdot}5$ h the flux at the bottom, where the concentration is u_{M0}, makes a step increase (from s_0 to $f(u_{M0}) > s > s_0$). This implies that the underflow concentration decreases by a step from u_{u0} to a value denoted by $u_u(2{\cdot}5 + 0)$,

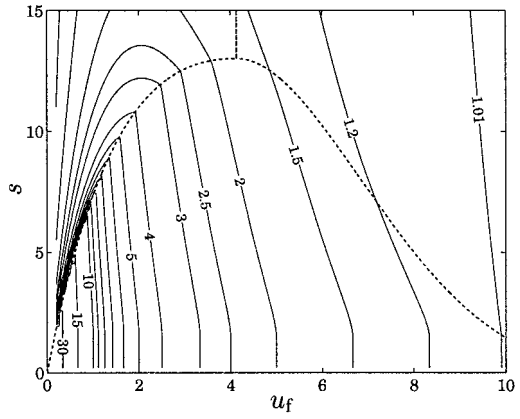

Figure 12. Operating chart with contours of the maximum thickening factor $\tilde{\theta}(u_f, s)$. The maximum of f_b is located at the concentration 2·06 kg/m^3.

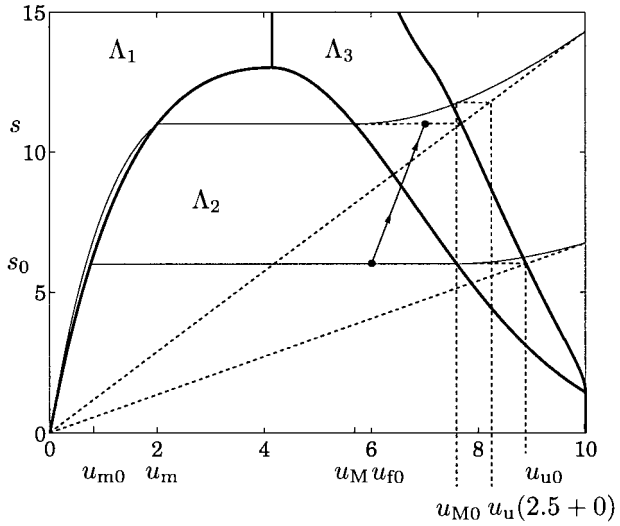

Figure 13. The path (with arrows) of the feed point in the control chart together with the graphs of $f_{lim}(\cdot, Q_{u0} = 1908)$ and $f_{lim}(\cdot, Q_u = 4045)$.

see Figure 13. After this time point the mass decreases since the feed flux is lower than the bottom flux. As characteristics carrying lower concentration values than u_{M0} reach the bottom (at $t \approx 5$ h) the bottom concentration decreases continuously. The new steady-state solution (which appears after infinite time) contains a sludge blanket with the concentration $u_m = 2{\cdot}0$ above and $u_M = 5{\cdot}7\ kg/m^3$ below it. The underflow concentration in the new steady state is $u_u = 7{\cdot}7$ kg/m^3, which is slightly higher than $u_{M0} = 7{\cdot}6$ kg/m^3, see Figure 13. Further simulation yields the new steady-state values $x_{sb} \approx 0{\cdot}9$ m and $m \approx 55$ tonnes. The settler is in optimal operation both in the initial and the final steady state. In Figure 9 we have shown the two corresponding points relating the mass in the settler and the depth of the sludge blanket.

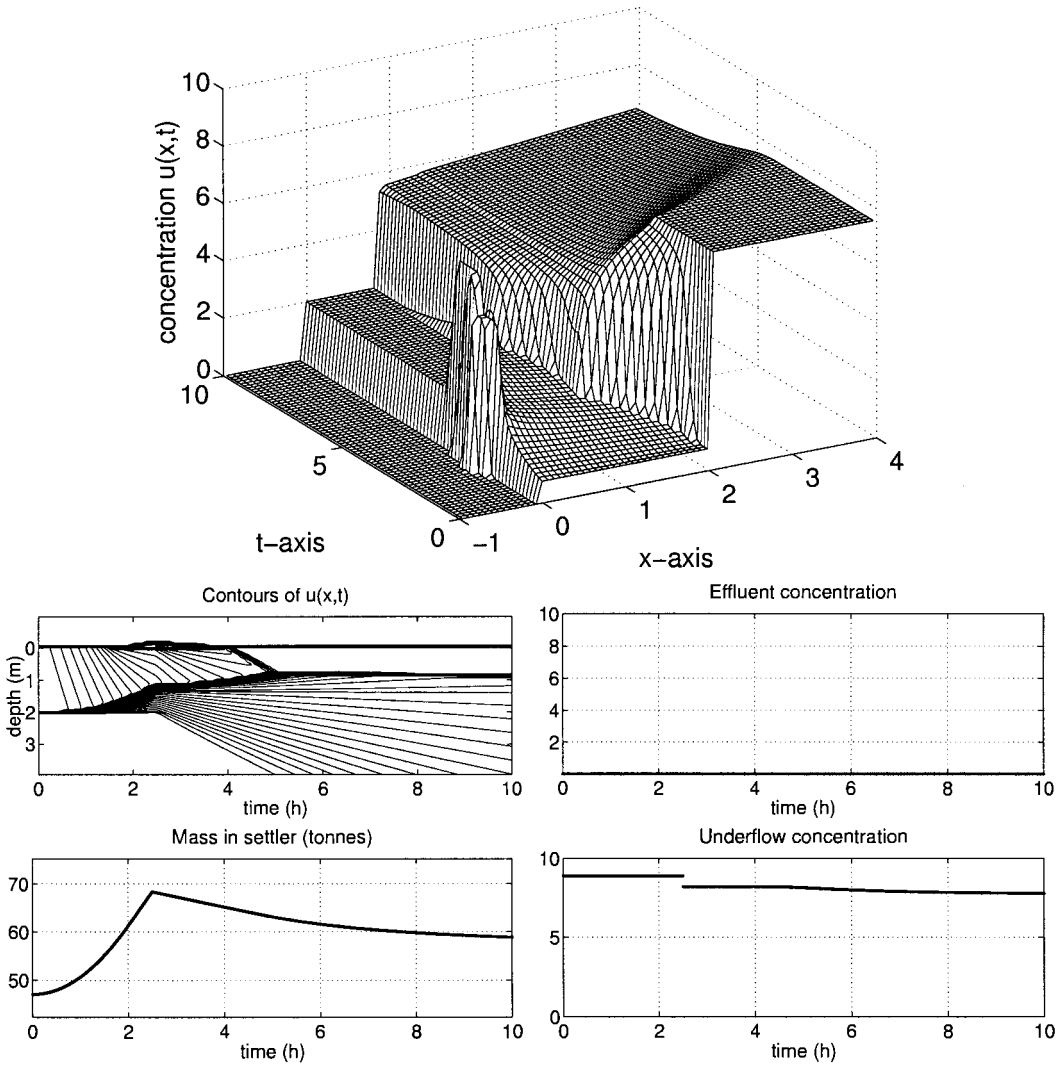

Figure 14. A numerical simulation with a control action at $t = 2.5$ h to prevent an overloaded settler.

6. Discussion and conclusions

The main types of nonlinearities of the process of continuous sedimentation are the following – at least when considered as a one-dimensional process:

1. The nonlinearity that causes large gradients (or discontinuities) of the concentration profile of the batch-sedimentation process originates from the nonlinear settling velocity as a function of the local concentration – the Kynch constitutive assumption. This leads to a hyperbolic partial differential equation (conservation law) with a convective nonlinear flux term.
2. Many suspensions show a nonlinear compressible behaviour at high concentrations. This can be modelled by adding a nonlinear (degenerate) diffusion term and hence the conservation law becomes (degenerate) parabolic. However, then numerical calculations are needed to obtain quantitative information.

3. The volume flows of the inlet and outlets of the clarifier-thickener unit cause another nonlinear phenomenon. Different flux functions in different regions imply spacial discontinuities of the flux function of the conservation law.

The paper deals only with the first and third type of nonlinearity for the following reasons:

- The Kynch assumption together with the conservation of mass in one dimension constitutes the solids-flux theory, which for many years has been, and still is, used to predict the behaviour of continuous sedimentation.
- Although based on the same assumptions, the results presented in the literature are not unique and do note cover all cases of loading conditions. The main reason for this has to do with the difficulty in concluding, by physical reasoning, the distribution of particles above and below the feed level (the third nonlinearity).
- The behaviour of a degenerate parabolic model for arbitrary loading conditions in continuous sedimentation is not yet analysed mathematically.
- Analytic calculations are possible in the hyperbolic case, generated by the first and third type of nonlinearity.

Mathematical results have now reached such a level that it is possible to describe the classical solids-flux theory rigorously and to extended it. Detailed information on the behaviour and the control of the process can be obtained. Because of the nonlinearities of the process, however, it is not easy to get a comprehensive overview of this information and a good sense of the process. One way is to visualise the information by means of engineering concepts such as graphical constructions and operating charts. In this paper all charts but one are concentration-flux diagrams in which the location of the feed point (u_f, s) yields different types of information.

The main results of the paper can be found in Sections 3.2 and 4. In Section 3.2 the type of steady-state solution, its concentrations and the total mass can be inferred from Figures 4–7. As for the graphical constructions for obtaining steady-state concentrations, we can establish that those made by Jernqvist [10, 11] (without any partial differential equations) agree with the present results. Formulae (8) comprise explicit expressions for the output variables $(u_\mathrm{e}, u_\mathrm{u}, Q_\mathrm{e})$ as functions of the feed variables (u_f, s) covering all steady states.

In Section 4 five purposes of the clarifier-thickener unit are discussed and formulated in terms of mathematical control criteria, which depend on the control variable Q_u. These criteria may be weighted together differently in different applications to form a control objective. There is a natural ideal control objective which says that the settler should be in optimal operation in steady state: zero concentration in the clarification zone and a large discontinuity (sludge blanket) within the thickening zone. The relation between the total mass, the depth of the sludge blanket and the concentrations above and below this during optimal operation can be enlightened graphically, see Figure 9. An important objective, which is necessary for obtaining optimal operation in steady state, is that the settler is critically loaded, *i.e.*, it is used at its maximum capacity with respect to the feed flux subject to the fact that there is no overflow of particles. Theorem 2 states that this objective can always be fulfilled and what the possible obtainable steady-state solutions are. Unfortunately, the control variable Q_u is only defined implicitly as a function of the feed variables. On the other hand, the location of the feed point in the operating charts for control in Figure 10 makes it easy to read the value of Q_u and the corresponding type of steady-state solution. Figure 11 visualises the variation with respect to the feed point of the maximum values of the effluent volume flow and underflow concentration, respectively, subject to the objective that the settler is critically

loaded. Similarly, Figure 12 shows the maximum value of the thickening factor, *i.e.*, the ratio of the underflow concentration to the feed concentration.

In this paper we have only defined optimal operation in *steady* state and we have only presented necessary conditions for obtaining this state. These conditions depend only on the feed point. To ensure optimal operation in steady state, the initial data as well as the dynamic behaviour need to be known in order to decide when to perform control actions. These issues will be analysed in a subsequent paper [51].

One other important extension of this paper would be to include the second type of nonlinearity mentioned above. For such a refined model analogous results can hopefully be obtained, yielding operating charts that would be more reliable for the operators of the plants. A further step would be to obtain analogous results for a two- or three-dimensional model – radial symmetry or rectangular tank, respectively – which takes flows in horizontal directions into account.

Acknowledgements

I am grateful to Dr Ulf Jeppsson, Lund Institute of Technology, and Dr Raimund Bürger, University of Stuttgart, for their comments on the manuscript. This work has been supported by the Swedish Research Council for Engineering Sciences (TFR), project 96-715.

Appendix A. Lemmas and proofs

LEMMA 1. *Let* $h(u) = f_{\mathrm{b}}(u) + \alpha u$ *for* $0 \le u \le u_{\max}$ *with* $\alpha \in \mathbb{R}$. *Then*

- $h'(u)u - h(u) < 0\,, \quad 0 < u < u_{\max}\,,$
- *the straight line* $y = \beta u$ *with* $\alpha < \beta < h'(0)$ *intersects the graph of* h *at precisely one point in* $(0, u_{\max})$.

Proof. Properties (1) of f_{b} imply that the continuously differentiable function $\varphi(u) = h'(u)u - h(u) = f_{\mathrm{b}}'(u)u - f_{\mathrm{b}}(u)$ satisfies $\varphi(0) = 0$, $\varphi(u_{\max}) = f_{\mathrm{b}}'(u_{\max})u_{\max} \le 0$ and $\varphi'(u) = f_{\mathrm{b}}''(u)u$, which is negative for $0 < u < u_{\mathrm{infl}}$ and positive for $u_{\mathrm{infl}} < u < u_{\max}$. It follows that $\varphi(u) < 0$ for $0 < u < u_{\max}$ and the first statement is proved. The second statement can be proved by setting $\psi(u) = (h(u) - \beta u)/u = f_{\mathrm{b}}(u)/u + (\alpha - \beta)$. This is a continuously differentiable function for $0 < u \le u_{\max}$ with the properties $\psi(0+) = h'(0) - \beta > 0$, $\psi(u_{\max}) = \alpha - \beta < 0$ and $\psi'(u) = \varphi(u)/u^2 < 0$ for $0 < u < u_{\max}$. Hence, there is a unique $u_1 \in (0, u_{\max})$ with $\psi(u_1) = 0 \Leftrightarrow h(u_1) = \beta u_1$, *i.e.*, there is a unique intersection in the interval $(0, u_{\max})$.

LEMMA 2. *The following properties hold:*

$$\frac{\mathrm{d}u_{\mathrm{M}}}{\mathrm{d}Q_{\mathrm{u}}} = \begin{cases} 0\,, & 0 \le Q_{\mathrm{u}} < \bar{Q}_{\mathrm{u}}\,, \\ -\dfrac{1}{Af_{\mathrm{b}}''(u_{\mathrm{M}})} < 0\,, & \bar{Q}_{\mathrm{u}} < Q_{\mathrm{u}} < \overline{\overline{Q}}_{\mathrm{u}}\,, \qquad \text{(see Figure 9)} \\ 0\,, & Q_{\mathrm{u}} > \overline{\overline{Q}}_{\mathrm{u}}\,, \end{cases} \tag{A1}$$

$$\frac{\mathrm{d}}{\mathrm{d}Q_\mathrm{u}} f\left(u_\mathrm{M}(Q_\mathrm{u}), Q_\mathrm{u}\right) = \frac{u_\mathrm{M}(Q_\mathrm{u})}{A}\,, \quad Q_\mathrm{u} \geq 0\,, \tag{A2}$$

$$\frac{\mathrm{d}u_\mathrm{m}}{\mathrm{d}Q_\mathrm{u}} \underset{=}{Q_\mathrm{u}\neq\overline{\overline{Q}}_\mathrm{u}} \frac{u_\mathrm{M}(Q_\mathrm{u}) - u_\mathrm{m}(Q_\mathrm{u})}{A f_\mathrm{b}'\left(u_\mathrm{m}(Q_\mathrm{u})\right) + Q_\mathrm{u}} \begin{cases} > 0\,, & 0 \leq Q_\mathrm{u} < \overline{\overline{Q}}_\mathrm{u}\,, \\ = 0\,, & Q_\mathrm{u} > \overline{\overline{Q}}_\mathrm{u}\,, \end{cases} \quad \text{(see Figure 9)} \tag{A3}$$

$$\frac{\partial f_\mathrm{lim}}{\partial Q_\mathrm{u}} = \begin{cases} \dfrac{u_\mathrm{f}}{A}\,, & u_\mathrm{f} \in \left(0, u_\mathrm{m}(Q_\mathrm{u})\right) \cup \left[u_\mathrm{M}(Q_\mathrm{u}), u_\mathrm{max}\right]\,, \\ \dfrac{u_\mathrm{M}(Q_\mathrm{u})}{A}\,, & u_\mathrm{f} \in \left(u_\mathrm{m}(Q_\mathrm{u}), u_\mathrm{M}(Q_\mathrm{u})\right)\,, \end{cases} \tag{A4}$$

$$\frac{\partial \mathcal{E}}{\partial Q_\mathrm{u}} = -\frac{\partial f_\mathrm{lim}}{\partial Q_\mathrm{u}} < 0\,, \quad \left(u_\mathrm{f}, s, Q_\mathrm{u}\right) \notin \left\{u_\mathrm{f} = u_\mathrm{m}(Q_\mathrm{u}), 0 \leq Q_\mathrm{u} < \overline{\overline{Q}}_\mathrm{u}\right\}\,, \tag{A5}$$

$$\frac{\partial u_\mathrm{u}}{\partial Q_\mathrm{u}} \begin{cases} = 0\,, & \left(u_\mathrm{f}, s, Q_\mathrm{u}\right) \in \left\{s > f_\mathrm{lim}(u_\mathrm{f}, Q_\mathrm{u}), u_\mathrm{m}(Q_\mathrm{u}) < u_\mathrm{f} \leq u_\mathrm{max}, 0 < Q_\mathrm{u} \leq \bar{Q}_\mathrm{u}\right\}\,, \\ < 0 \quad \text{a.e.}\,, & \text{otherwise}\,. \end{cases} \tag{A6}$$

Proof; For $\bar{Q}_\mathrm{u} < Q_\mathrm{u} < \overline{\overline{Q}}_\mathrm{u}$ the definition of the local minimizer u_M gives

$$\frac{\partial f}{\partial u}\left(u_\mathrm{M}(Q_\mathrm{u}), Q_\mathrm{u}\right) = 0 \quad \Longleftrightarrow \quad f_\mathrm{b}'\left(u_\mathrm{M}(Q_\mathrm{u})\right) + \frac{Q_\mathrm{u}}{A} = 0\,. \tag{A7}$$

Hence (A1) follows. For all values of $Q_\mathrm{u} \geq 0$ except $\bar{Q}_\mathrm{u}$ and $\overline{\overline{Q}}_\mathrm{u}$ we have

$$\begin{aligned} \frac{\mathrm{d}}{\mathrm{d}Q_\mathrm{u}} f\left(u_\mathrm{M}(Q_\mathrm{u}), Q_\mathrm{u}\right) &= \frac{\mathrm{d}}{\mathrm{d}Q_\mathrm{u}} \left(f_\mathrm{b}\left(u_\mathrm{M}(Q_\mathrm{u})\right) + \frac{Q_\mathrm{u}}{A} u_\mathrm{M}(Q_\mathrm{u}) \right) = \\ &= \left(f_\mathrm{b}'\left(u_\mathrm{M}(Q_\mathrm{u})\right) + \frac{Q_\mathrm{u}}{A} \right) \frac{\mathrm{d}u_\mathrm{M}}{\mathrm{d}Q_\mathrm{u}} + \frac{u_\mathrm{M}(Q_\mathrm{u})}{A}\,. \end{aligned}$$

The first term here is zero. This is because (A7) holds for $\bar{Q}_\mathrm{u} < Q_\mathrm{u} < \overline{\overline{Q}}_\mathrm{u}$, and because $\frac{\mathrm{d}u_\mathrm{M}}{\mathrm{d}Q_\mathrm{u}} = 0$ holds for $Q_\mathrm{u} \in [0, \bar{Q}_\mathrm{u}) \cup (\overline{\overline{Q}}_\mathrm{u}, \infty)$. By continuity (A2) holds for all $Q_\mathrm{u} \geq 0$. The dependence of u_m on Q_u for $Q_\mathrm{u} < \overline{\overline{Q}}_\mathrm{u}$ is given implicitly by

$$f\left(u_\mathrm{m}(Q_\mathrm{u}), Q_\mathrm{u}\right) = f\left(u_\mathrm{M}(Q_\mathrm{u}), Q_\mathrm{u}\right) \quad \Longleftrightarrow \quad f_\mathrm{b}\left(u_\mathrm{m}(Q_\mathrm{u})\right) + \frac{Q_\mathrm{u}}{A} u_\mathrm{m}(Q_\mathrm{u}) = f\left(u_\mathrm{M}(Q_\mathrm{u}), Q_\mathrm{u}\right)\,.$$

Differentiation with respect to Q_u and using (A2) we obtain (A3), where the denominator is equal to $A\frac{\partial f}{\partial u}\left(u_\mathrm{m}(Q_\mathrm{u}), Q_\mathrm{u}\right) > 0$ for $Q_\mathrm{u} < \bar{Q}_\mathrm{u}$. (A4) and (A5) are straightforward to obtain by using (A2). Differentiation of the underflow concentration (13) yields $\partial u_\mathrm{u}/\partial Q_\mathrm{u} = -As/Q_\mathrm{u}^2 < 0$ for $s < f_\mathrm{lim}(u_\mathrm{f}, Q_\mathrm{u})$. For $s > f_\mathrm{lim}(u_\mathrm{f}, Q_\mathrm{u})$ and $u_\mathrm{f} \in (0, u_\mathrm{m}(Q_\mathrm{u})) \cup \left[u_\mathrm{M}(Q_\mathrm{u}), u_\mathrm{max}\right]$ we have

$$\frac{\partial u_\mathrm{u}}{\partial Q_\mathrm{u}} = -\frac{A f_\mathrm{lim}}{Q_\mathrm{u}^2} + \frac{A}{Q_\mathrm{u}} \frac{\partial f_\mathrm{lim}}{\partial Q_\mathrm{u}} = -\frac{A f\left(u_\mathrm{f}, Q_\mathrm{u}\right)}{Q_\mathrm{u}^2} + \frac{u_\mathrm{f}}{Q_\mathrm{u}} = -\frac{A f_\mathrm{b}(u_\mathrm{f})}{Q_\mathrm{u}^2}\,,$$

which is negative unless $u_\mathrm{f} = u_\mathrm{max}$. Similarly, for $s > f_\mathrm{lim}(u_\mathrm{f}, Q_\mathrm{u})$ and $u_\mathrm{m}(Q_\mathrm{u}) < u_\mathrm{f} < u_\mathrm{M}(Q_\mathrm{u})$ we get

$$\frac{\partial u_\mathrm{u}}{\partial Q_\mathrm{u}} = -\frac{A f_\mathrm{b}\,(u_\mathrm{M}(Q_\mathrm{u}))}{Q_\mathrm{u}^2} \begin{cases} = -\dfrac{A f_\mathrm{b}(u_\mathrm{max})}{Q_\mathrm{u}^2} = 0\,, & 0 < Q_\mathrm{u} \le \bar{Q}_\mathrm{u}\,, \\ < 0\,, & Q_\mathrm{u} > \bar{Q}_\mathrm{u}\,. \end{cases}$$

We note that the derivative $\partial u_\mathrm{u}/\partial Q_\mathrm{u}$ is not defined on the null sets (surfaces) $\{(u_\mathrm{f}, s, Q_\mathrm{u}) : s > f_\mathrm{lim}(u_\mathrm{f}, Q_\mathrm{u}), u_\mathrm{f} = u_\mathrm{m}(Q_\mathrm{u})\} = \{(u_\mathrm{m}(Q_\mathrm{u}), s, Q_\mathrm{u}) : s > f\,(u_\mathrm{m}(Q_\mathrm{u}), Q_\mathrm{u})\}$ and $\{(u_\mathrm{f}, s, Q_\mathrm{u}) : s = f_\mathrm{lim}(u_\mathrm{f}, Q_\mathrm{u})\}$. (A6) is proved.

Proof of Theorem 2. It is easy to see that $\mathcal{E}(u_\mathrm{f}, s, Q_\mathrm{u})$ is a continuous function on $\Omega \times \{Q_\mathrm{u} \ge 0\}$. For a given $(u_\mathrm{f}, s) \in \Omega$ we have $\mathcal{E}(u_\mathrm{f}, s, 0) = s > 0$, $\lim_{Q_\mathrm{u}\to\infty} \mathcal{E}(u_\mathrm{f}, s, Q_\mathrm{u}) = \lim_{Q_\mathrm{u}\to\infty} (s - f(u_\mathrm{f}, Q_\mathrm{u})) = -\infty$, and (A5) implies that $\mathcal{E}(u_\mathrm{f}, s, \cdot)$ is strictly decreasing. Hence there exists a unique $Q_\mathrm{u} = \tilde{Q}_\mathrm{u}$ such that $\mathcal{E}(u_\mathrm{f}, s, \tilde{Q}_\mathrm{u}) = 0$. These arguments also imply (12) and the continuity of $\tilde{Q}_\mathrm{u}(u_\mathrm{f}, s)$ (the implicit-function theorem without differentiability). The fact that $(u_\mathrm{f}, s) \in \ell_1(\tilde{Q}_\mathrm{u})$ etc. is a direct consequence of the definition of Λ_1, etc. With the help of Lemma 2 we can differentiate the identity $s = f_\mathrm{lim}\left(u_\mathrm{f}, s, \tilde{Q}_\mathrm{u}(u_\mathrm{f}, s)\right)$ with respect to u_f to obtain

$$0 = \begin{cases} \dfrac{\partial f}{\partial u}(u_\mathrm{f}, \tilde{Q}_\mathrm{u}) + \dfrac{u_\mathrm{f}}{A}\dfrac{\partial \tilde{Q}_\mathrm{u}}{\partial u_\mathrm{f}}\,, & u_\mathrm{f} \in \left(0, u_\mathrm{m}(\tilde{Q}_\mathrm{u})\right) \cup \left(u_\mathrm{M}(\tilde{Q}_\mathrm{u}), u_\mathrm{max}\right], \\ \dfrac{u_\mathrm{M}(\tilde{Q}_\mathrm{u})}{A}\dfrac{\partial \tilde{Q}_\mathrm{u}}{\partial u_\mathrm{f}}\,, & u_\mathrm{f} \in \left(u_\mathrm{m}(\tilde{Q}_\mathrm{u}), u_\mathrm{M}(\tilde{Q}_\mathrm{u})\right)\,, \end{cases}$$

and with respect to s to obtain

$$1 = \frac{\partial f_\mathrm{lim}}{\partial Q_\mathrm{u}}\frac{\partial \tilde{Q}_\mathrm{u}}{\partial s} = \begin{cases} \dfrac{u_\mathrm{f}}{A}\dfrac{\partial \tilde{Q}_\mathrm{u}}{\partial s}\,, & u_\mathrm{f} \in \left(0, u_\mathrm{m}(\tilde{Q}_\mathrm{u})\right) \cup \left(u_\mathrm{M}(\tilde{Q}_\mathrm{u}), u_\mathrm{max}\right], \\ \dfrac{u_\mathrm{M}(\tilde{Q}_\mathrm{u})}{A}\dfrac{\partial \tilde{Q}_\mathrm{u}}{\partial s}\,, & u_\mathrm{f} \in \left(u_\mathrm{m}(\tilde{Q}_\mathrm{u}), u_\mathrm{M}(\tilde{Q}_\mathrm{u})\right)\,, \end{cases}$$

from which the properties of the derivatives follow. Note the continuity as $u_\mathrm{f} = u_\mathrm{M}(Q_\mathrm{u})$, *i.e.*, over the boundary between Λ_2 and Λ_3. The last statement of the theorem is proved similarly. (A1) implies that $f\,(u_\mathrm{M}(Q_\mathrm{u}), Q_\mathrm{u})$ is a continuous and increasing function of Q_u with $f\,(u_\mathrm{M}(0), 0) = f(u_\mathrm{max}, 0) = 0$ and $\lim_{Q_\mathrm{u}\to\infty} f\,(u_\mathrm{M}(Q_\mathrm{u}), Q_\mathrm{u}) = \lim_{Q_\mathrm{u}\to\infty} f\,(u_\mathrm{infl}, Q_\mathrm{u}) = \infty$. Hence, for given $(u_\mathrm{f}, s) \in \Lambda_3$ there exists a unique $Q_\mathrm{u} > 0$ such that $f\,(u_\mathrm{M}(Q_\mathrm{u}), Q_\mathrm{u}) = s$, *i.e.*, $(u_\mathrm{f}, s) \in \ell_3(Q_\mathrm{u})$.

Proof of (14a):

$$\frac{\partial \tilde{Q}_\mathrm{e}}{\partial u_\mathrm{f}} = -\frac{As}{u_\mathrm{f}^2} - \frac{\partial \tilde{Q}_\mathrm{u}}{\partial u_\mathrm{f}}\,.$$

The latter derivative is given by Theorem 2. Hence $\partial \tilde{Q}_\mathrm{e}/\partial u_\mathrm{f} = -As/u_\mathrm{f}^2 < 0$ for $(u_\mathrm{f}, s) \in \Lambda_2$. For $(u_\mathrm{f}, s) \notin \Lambda_2 \cup P_1$ the fact that $s = f_\mathrm{lim}(u_\mathrm{f}, \tilde{Q}_\mathrm{u}) = f(u_\mathrm{f}, \tilde{Q}_\mathrm{u})$ together with Lemma 1 implies

$$\frac{\partial \tilde{Q}_\mathrm{e}}{\partial u_\mathrm{f}} = -\frac{As}{u_\mathrm{f}^2} - \frac{A}{u_\mathrm{f}}\frac{\partial f}{\partial u}(u_\mathrm{f}, \tilde{Q}_\mathrm{u}) = -\frac{A}{u_\mathrm{f}}\left(\frac{f(u_\mathrm{f}, \tilde{Q}_\mathrm{u})}{u_\mathrm{f}} - \frac{\partial f}{\partial u}(u_\mathrm{f}, \tilde{Q}_\mathrm{u})\right) < 0\,.$$

Proof of (14b):

$$\frac{\partial \tilde{Q}_\mathrm{e}}{\partial s} = \frac{A}{u_\mathrm{f}} - \frac{\partial \tilde{Q}_\mathrm{u}}{\partial s} = \begin{cases} 0\,, & (u_\mathrm{f}, s) \notin \Lambda_2 \cup P_1\,, \\ \dfrac{A}{u_\mathrm{f}} - \dfrac{A}{u_\mathrm{M}(\tilde{Q}_\mathrm{u})}\,, & (u_\mathrm{f}, s) \in \Lambda_2\,. \end{cases}$$

Since $u_\mathrm{f} = u_\mathrm{M}(\tilde{Q}_\mathrm{u})$ on the boundary between Λ_2 and Λ_4, the derivative is zero on the slightly larger set $\Lambda_1 \cup \mathrm{closure}(\Lambda_4)$. It is positive in the interior of Λ_2, since $u_\mathrm{f} < u_\mathrm{M}(\tilde{Q}_\mathrm{u})$ there.
Proof of (14c): $u_\mathrm{f} = u_\mathrm{max}$ implies

$$\tilde{Q}_\mathrm{e}(u_\mathrm{max}, s) = \frac{A f_\mathrm{lim}(u_\mathrm{max}, \tilde{Q}_\mathrm{u})}{u_\mathrm{max}} - \tilde{Q}_\mathrm{u} = \frac{A\frac{\tilde{Q}_\mathrm{u}}{A} u_\mathrm{max}}{u_\mathrm{max}} - \tilde{Q}_\mathrm{u} = 0.$$

This fact together with (14a) and the continuity of $\tilde{Q}_\mathrm{e}$ implies (14c).
Property (14d) follows directly from Theorem 2.
Proof of (14f): $u_\mathrm{f} = u_\mathrm{max}$ implies

$$\tilde{u}_\mathrm{u}(u_\mathrm{max}, s) = \frac{A f_\mathrm{lim}(u_\mathrm{max}, \tilde{Q}_\mathrm{u})}{\tilde{Q}_\mathrm{u}} = \frac{A\frac{\tilde{Q}_\mathrm{u}}{A} u_\mathrm{max}}{\tilde{Q}_\mathrm{u}} = u_\mathrm{max}\,. \tag{A8}$$

For $(u_\mathrm{f}, s) \in \Lambda_2 \cap \left\{(u, y) : y \le \bar{q}_\mathrm{u} u_\mathrm{max}\right\}$ we have $\tilde{Q}_\mathrm{u} \le \bar{Q}_\mathrm{u}$, which implies $u_\mathrm{M}(\tilde{Q}_\mathrm{u}) = u_\mathrm{max}$ and $s = f_\mathrm{lim}(u_\mathrm{max}, \tilde{Q}_\mathrm{u})$. As in (A8), $\tilde{u}_\mathrm{u} = u_\mathrm{max}$ follows. Hence, $\tilde{u}_\mathrm{u} = u_\mathrm{max}$ in Υ. For other feed points $0 < s = f_\mathrm{lim}(u_\mathrm{f}, \tilde{Q}_\mathrm{u}) < f(u_\mathrm{max})$ holds, which implies $0 < \tilde{u}_\mathrm{u} = As/\tilde{Q}_\mathrm{u} < Af(u_\mathrm{max})/\tilde{Q}_\mathrm{u} = u_\mathrm{max}$.
Proof of (14e): (14f) implies that $\partial \tilde{u}_\mathrm{u}/\partial s = 0$ holds in Υ. For $(u_\mathrm{f}, s) \in \Lambda_2 \setminus \Upsilon$ we have $\tilde{Q}_\mathrm{u} > \bar{Q}_\mathrm{u}$, $u_\mathrm{M}(\tilde{Q}_\mathrm{u}) < u_\mathrm{max}$, thus $f_\mathrm{b}\left(u_\mathrm{M}(\tilde{Q}_\mathrm{u})\right) > 0$. Theorem 2 and the fact that $s = f\left(u_\mathrm{M}(\tilde{Q}_\mathrm{u})\right) = f_\mathrm{b}\left(u_\mathrm{M}(\tilde{Q}_\mathrm{u})\right) + \tilde{Q}_\mathrm{u} u_\mathrm{M}(\tilde{Q}_\mathrm{u})/A$ yield

$$\frac{\partial \tilde{u}_\mathrm{u}}{\partial s} = \frac{A}{\tilde{Q}_\mathrm{u}}\left(1 - \frac{s}{\tilde{Q}_\mathrm{u}}\frac{\partial \tilde{Q}_\mathrm{u}}{\partial s}\right) = \frac{A}{\tilde{Q}_\mathrm{u}}\left(1 - \frac{sA}{\tilde{Q}_\mathrm{u} u_\mathrm{M}(\tilde{Q}_\mathrm{u})}\right) = -\frac{A f_\mathrm{b}\left(u_\mathrm{M}(\tilde{Q}_\mathrm{u})\right)}{\tilde{Q}_\mathrm{u} u_\mathrm{M}(\tilde{Q}_\mathrm{u})} < 0\,.$$

For $(u_\mathrm{f}, s) \notin \Lambda_2 \cup P_1$ we have

$$\frac{\partial \tilde{u}_\mathrm{u}}{\partial s} = \frac{A}{\tilde{Q}_\mathrm{u}}\left(1 - \frac{sA}{\tilde{Q}_\mathrm{u} u_\mathrm{f}}\right) = -\frac{A\tilde{Q}_\mathrm{e}}{\tilde{Q}_\mathrm{u}^2} \begin{cases} < 0\,, & u_\mathrm{f} < u_\mathrm{max}\,, \\ = 0\,, & u_\mathrm{f} = u_\mathrm{max}\,, \end{cases}$$

by (14c). (14e) is proved.
Proof of (15a): We differentiate $\tilde{\theta} = As/(\tilde{Q}_\mathrm{u} u_\mathrm{f})$ and obtain

$$\frac{\partial \tilde{\theta}}{\partial u_\mathrm{f}} = -\frac{As}{\tilde{Q}_\mathrm{u}^2 u_\mathrm{f}}\frac{\partial \tilde{Q}_\mathrm{u}}{\partial u_\mathrm{f}} - \frac{As}{\tilde{Q}_\mathrm{u} u_\mathrm{f}^2}\,.$$

Theorem 2 and the fact that $\partial f/\partial u(u_\mathrm{f}, \tilde{Q}_\mathrm{u}) = f_\mathrm{b}'(u_\mathrm{f}) + \tilde{Q}_\mathrm{u}/A$ imply (15a).
Property (15b) follows from (14e).

References

1. H. S. Coe and G. H. Clevenger, Methods for determining the capacities of slime-settling tanks. *Trans. AIME* 55 (1916) 356–384.

2. P. A. Vesilind, Theoretical considerations: Design of prototype thickeners. *Water and Sewage Works* 115 (1968) 302–307.
3. F. Concha and A. Barrientos, A critical review of thickener design methods. *KONA* 11 (1993) 79–104.
4. G. J. Kynch, A theory of sedimentation. *Trans. Faraday Soc.* 48 (1952) 166–176.
5. P. T. Shannon, E. Stroupe and E. M. Tory, Batch and continuous thickening. *Ind. Eng. Chem. Fundam.* 2 (1963) 203–211.
6. K. E. Davis, W. B. Russel and W. J. Glantschnig, Settling suspensions of colloidal silica: Observations and X-ray measurements. *J. Chem. Soc. Faraday Trans.* 87 (1991) 411–424.
7. D. Chang, T. Lee, Y. Jang, M. Kim and S. Lee, Non-colloidal sedimentation compared with Kynch theory. *Powder Technol* 92 (1997) 81–87.
8. N. Yoshioka, Y. Hotta, S. Tanaka, S. Naito and S. Tsugami, Continuous thickening of homogeneous flocculated slurries. *Kagagi Kogaku (Chem. Eng. Tokyo)* 21 (1957) 66–74.
9. Å. Jernqvist, Experimental and theoretical studies of thickeners. Part 1. Derivation of basic equations and basic graphical constructions. *Svensk Papperstidning* 68 (1965) 506–511.
10. Å. Jernqvist, Experimental and theoretical studies of thickeners. Part 2. Graphical calculation of thickener capacity. *Svensk Papperstidning* 68 (1965) 545–548.
11. Å. Jernqvist, Experimental and theoretical studies of thickeners. Part 3. Concentration distribution of the steady and unsteady stat operation of thickeners. *Svensk Papperstidning* 68 (1965) 578–582.
12. N. J. Hasset, Concentrations in a continuous thickener. *Ind. Chem.* 40 (1964) 29–33.
13. R. I. Dick, Role of activated sludge final settling tanks. *J. San. Eng. Div.* 63(SA2) (1970) 423–436.
14. W. H. McHarg, Designing the optimum system for biological waste-treatment. *Chem. Eng.* 80 (1973) 46–49.
15. Å. Jernqvist, Experimental and theoretical studies of thickeners. Part 4. Experimental results. *Svensk Papperstidning* 69 (1966) 395–398.
16. P. T. Shannon and E. M. Tory, The analysis of continuous thickening. *SME Trans.* 235 (1966) 375–382.
17. P. A. Vesilind, *Treatment and Disposal of Wastewater Sludges*. Ann Arbor Science Pub., Inc., Ann Arbor, Michigan, USA (1974) 236 pp.
18. L. G. Eklund and Å. Jernqvist, Experimental study of the dynamics of a vertical continuous thickener–I. *Chem. Eng. Sci.* 30 (1975) 597–605.
19. R. I. Dick, Folklore in the design of final settling tanks. *J. Water Pollut. Control Fed.* 48 (1976) 633–644.
20. T. M. Keinath, M. Ryckman, C. Dana and D. Hofer, Activated sludge – unified system design and operation. *J. Envir. Eng. Div. ASCE* 103(EE5) (1977) 829–849.
21. V. D. Laquidara and T. M. Keinath, Mechanism of clarification failure. *J. Water Pollut. Control Fed.* 55 (1983) 54–57.
22. T. M. Keinath, Operational dynamics and control of secondary clarifiers. *J. Water Pollut. Control Fed.* 57 (1985) 770–776.
23. O. Lev, E. Rubin and M. Sheintuch, Steady state analysis of a continuous clarifier-thickener system. *AIChE J.* 32 (1986) 1516–1525.
24. M. Smollen and G. A. Ekama, Comparison of empirical settling-velocity equations in flux theory for secondary settling tanks. *Water SA* 10 (1984) 175–183.
25. G. A. Ekama and G. V. R. Marais, Sludge settlability and secondary settling tank design procedures. *Water Pollut. Control* 85 (1986) 101–113.
26. M. Sheintuch, Steady state modelling of reactor-settler interaction. *Water Res.* 21 (1987) 1463–1472.
27. J. B. Christian, Improve clarifier and thickener design and operation. *Chem. Eng. Prog.* 90 (1994) 50–56.
28. P. Balslev, C. Nickelsen and A. Lynggaard-Jensen, On-line flux-theory based control of secondary clarifiers. *Water Sci. Tech.* 30 (1994) 209–218.
29. A. E. Ozinsky, G. A. Ekama and B. D. Reddy, Mathematical simulation of dynamic behaviour of secondary settling tanks. Technical Report W85, Dept of Civil Engineering, University of Cape Town (1994).
30. A. E. Ozinsky and G. A. Ekama, Secondary settling tank modeling and design part 1: Review of theoretical and practical developments. *Water SA* 21 (1995) 325–332.
31. T. Matko, N. Fawcett, A. Sharpe and T. Stephenson, Recent progress in the numerical modelling of wastewater sedimentation tanks. *Trans. I. Chem. E.* 74(B) (1996) 245–258.
32. P. D. Lax, Hyperbolic systems of conservation laws II. *Comm. Pure Appl. Math.* 10 (1957) 537–566.
33. O. A. Oleinik, Uniqueness and stability of the generalized solution of the Cauchy problem for a quasi-linear equation. *Uspekhi Mat. Nauk* 14 (1959) 165–170, Amer. Math. Soc. Trans. Ser. 2, 33 (1964) 285–290.

34. C. A. Petty, Continuous sedimentation of a suspension with a nonconvex flux law. *Chem. Eng. Sci.* 30 (1975) 1451–1458.
35. H. K. Rhee, R. Aris and N. Amundson, *First-Order Partial Differential Equations* Volume 1. Englewood Cliffs: Prentice Hall, (1986) 543 pp.
36. M. C. Bustos and F. Concha, On the construction of global weak solutions in the Kynch theory of sedimentation. *Math. Methods Appl. Sci.* 10 (1988) 245–264.
37. M. C. Bustos, F. Concha and W. Wendland, Global weak solutions to the problem of continuous sedimentation of an ideal suspension. *Math. Methods Appl. Sci.* 13 (1990) 1–22.
38. M. C. Bustos, F. Paiva and W. Wendland, Control of continuous sedimentation as an initial and boundary value problem. *Math. Methods Appl. Sci.* 12 (1990) 533–548.
39. S. Diehl, G. Sparr and G. Olsson, Analytical and numerical description of the settling process in the activated sludge operation. In R. Briggs, editor, *Instrumentation, Control and Automation of Water and Wastewater Treatment and Transport Systems*, pages 471–478. IAWPRC, Pergamon Press (1990).
40. J.-Ph. Chancelier, M. Cohen de Lara and F. Pacard, Analysis of a conservation PDE with discontinuous flux: A model of settler. *SIAM J. Appl. Math.* 54 (1994) 954–995.
41. S. Diehl, On scalar conservation laws with point source and discontinuous flux funtion. *SIAM J. Math. Anal.* 26 (1995) 1425–1451.
42. S. Diehl, A conservation law with point source and discontinuous flux funtion modelling continuous sedimentation. *SIAM J. Appl. Math.* 56 (1996) 388–419.
43. J.-Ph. Chancelier, M. Cohen de Lara, C. Joannis and F. Pacard, New insight in dynamic modelling of a secondary settler – I. Flux theory and steady-states analysis. *Water Res.* 31 (1997) 1847–1856.
44. S. Diehl, On boundary conditions and solutions for ideal clarifier-thickener units. *Chem. Eng. J.* 80 (2000) 119–133.
45. S. Diehl, Scalar conservation laws with discontinuous flux funtion: I. The viscous profile condition. *Comm. Math. Phys.* 176 (1996) 23–44.
46. S. Diehl and N.-O. Wallin, Scalar conservation laws with discontinuous flux function: II. On the stability of the viscous profiles. *Comm. Math. Phys.* 176 (1996) 45–71.
47. S. Diehl, Dynamic and steady-state behaviour of continuous sedimentation. *SIAM J. Appl. Math.* 57 (1997) 991–1018.
48. R. Bürger and F. Concha, Mathematical model and numerical simulation of the settling of flocculated suspensions. *Int. J. Multiphase Flow* 24 (1998) 1005–1023.
49. R. Bürger, W. L. Wendland and F. Concha, Model equations for gravitational sedimentation-consolidation processes. *Z. Angew. Math. Mech.* 80 (2000) 79–92.
50. M. C. Bustos, F. Concha, R. Bürger and E. M. Tory, *Sedimentation and Thickening: Phenomenlogical Foundation and Mathematical Theory*. Dordrecht: Kluwer Academic Publishers (1999) 285 pp.
51. S. Diehl, Operating charts for continuous sedimentation II: Step responses and dynamic control. In preparation (2001).
52. F. M. Auzerais, R. Jackson, W. B. Russel and W. F. Murphy, The transient settling of stable and flocculated dispersions. *J. Fluid Mech.* 221 (1990) 613–639.
53. P. A. Vesilind and G. N. Jones, A reexamination of the batch-thickening curve. *Res. J. Water Pollut. Control Fed.* 62 (1990) 887–893.
54. R. Bürger and E. M. Tory, On upper rarefaction waves in batch settling. *Powder Technol.* 108 (2000) 74–87.
55. S. Diehl and U. Jeppsson, A model of the settler coupled to the biological reactor. *Water Res.* 32 (1998) 331–342.